---

**Article:**
Humes, JR orcid.org/0000-0002-1407-7880, Schiffrin, B, Calabrese, AN et al. (4 more authors) (2019) The Role of SurA PPIase Domains in Preventing Aggregation of the Outer Membrane Proteins tOmpA and OmpT. Journal of Molecular Biology, 431 (6). pp. 1267-1283. ISSN 0022-2836

https://doi.org/10.1016/j.jmb.2019.01.032

---

# The Role of SurA PPIase Domains in Preventing Aggregation of the Outer Membrane Proteins tOmpA and OmpT

Julia R. Humes[1,†], Bob Schiffrin[1,†], Antonio N. Calabrese[1], Anna J. Higgins[1], David R. Westhead[1], David J. Brockwell[1,*], Sheena E. Radford[1,*]

1 - Astbury Centre for Structural Molecular Biology, School of Molecular and Cellular Biology, Faculty of Biological Sciences, University of Leeds, Leeds LS2 9JT, UK

† These authors contributed equally to this work

* Corresponding authors: d.j.brockwell@leeds.ac.uk (tel: +44 113 343 7821); s.e.radford@leeds.ac.uk (tel: +44 113 343 3170)

**Keywords**: Outer membrane protein, chaperone, aggregation, prolyl isomerase, SurA

**Abbreviations**: OMP, outer membrane protein; PPIase, peptidyl prolyl isomerase; SurA ΔP2, SurA in which PPIase domain P2 has been deleted; SurA N-Ct, SurA in which both PPIase domains P1 and P2 are deleted; BAM, β-barrel assembly machinery.

**Abstract**

SurA is a conserved ATP-independent periplasmic chaperone involved in the biogenesis of outer membrane proteins (OMPs). *E. coli* SurA has a core domain and two peptidyl prolyl isomerase (PPIase) domains, the role(s) of which remain unresolved. Here we show that while SurA homologues in early proteobacteria typically contain one or no PPIase domains, the presence of two PPIase domains is common in SurA in later proteobacteria, implying an evolutionary advantage for this domain architecture. Bioinformatics analysis of >350,000 OMP sequences showed that their length, hydrophobicity and aggregation propensity is similar across the proteobacterial classes, ruling out a simple correlation between SurA domain architecture and these properties of OMP sequences. To investigate the role of the PPIase domains in SurA activity we deleted one or both PPIase domains from *E.coli* SurA and investigated the ability of the resulting proteins to bind and prevent the aggregation of tOmpA (19 kDa) and OmpT (33 kDa). The results show that wild-type SurA inhibits the aggregation of both OMPs, as do the cytoplasmic OMP chaperones trigger factor and SecB. However, while the ability of SurA to bind and prevent tOmpA aggregation does not depend on its PPIase domains, deletion of even a single PPIase domain ablates the ability of SurA to prevent OmpT aggregation. The results demonstrate that the core domain of SurA endows its generic chaperone ability, while the presence of PPIase domains enhances its chaperone activity for specific OMPs, suggesting one reason for the conservation of multiple PPIase domains in SurA in proteobacteria.

**Graphical Abstract**

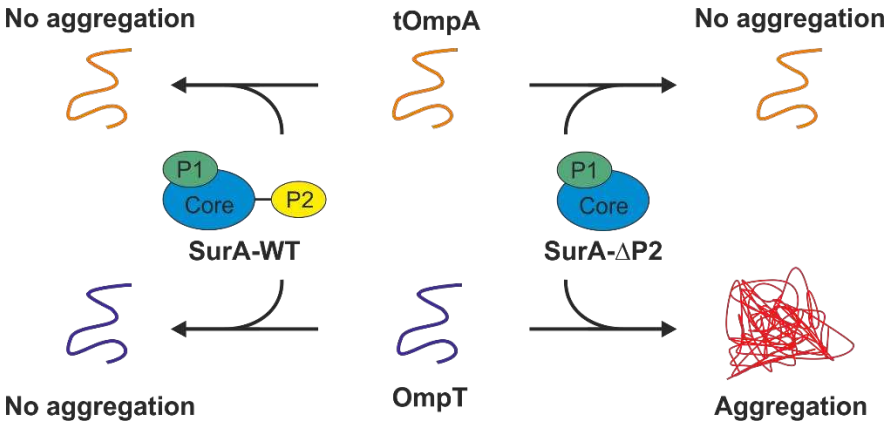


**Highlights:**

- The role(s) of the two PPIase domains in *E. coli* SurA remain unresolved
- Multiple SurA PPIase domains are conserved in β- and γ-proteobacteria
- OMP sequence properties do not reveal a correlation with SurA domain architecture
- tOmpA and OmpT require different SurA domains for chaperoning
- SurA-OMP specificity suggests one reason for multiple PPIase domain conservation

## Introduction

The survival and pathogenesis of Gram-negative bacteria depend on the correct assembly of the outer membrane (OM) [1-3]. This highly specialised membrane is densely packed with β-barrel outer membrane proteins (OMPs) which carry out a multitude of essential functions, and include transporters, enzymes, adhesins and secretory channels [4-6]. The biogenesis of β-barrel outer membrane proteins (OMPs) involves transportation from their site of synthesis in the cytoplasm to the β-barrel assembly machinery (BAM) for insertion into the OM [7]. This process requires a network of molecular chaperones. Nascent OMPs first interact with Trigger Factor (TF) and subsequently with SecB which aids in OMP delivery to the SecYEG complex

for translocation across the inner membrane [8]. Once in the periplasm, these aggregation-prone proteins interact with chaperones including Skp, SurA, FkpA and DegP which maintain OMPs in a folding-competent state, enabling them to traverse the aqueous periplasmic space [6, 9]. Periplasmic chaperones carry out their function in an environment devoid of ATP [10] and so must prevent aggregation and enhance folding using mechanism(s) distinct from those of ATP-dependent chaperones [11]. On reaching the OM, OMPs interact with the BAM complex which promotes their insertion into the OM and folding to their native states [12-18]. Evidence from *in vivo* work suggests that SurA may be involved in direct delivery of OMP substrates to BAM [19-23], although the molecular mechanism by which this occurs remains unresolved.

SurA is conserved across proteobacteria [24] and has been shown to play a key role in OMP biogenesis [20, 22, 25-28]. In *E. coli,* deletion of SurA leads to depleted levels of a number of OMPs in the OM [25, 27], accumulation of unfolded proteins in the periplasm, upregulation of the $\sigma^E$ stress response, and reduced antibiotic resistance [29-31]. SurA has also been shown to be involved in pathogenicity, with roles in the correct assembly of virulence factors such as pili [29, 32] and adhesins [33]. Structurally, *E. coli* SurA consists of a core region made up of an N-terminal domain and a short C-terminal domain, separated in primary sequence by two parvulin-like peptidylprolyl isomerase (PPIase) domains (P1 and P2) (**Fig. 1a**) [34]. The functional mechanism(s) of SurA, including the roles of the core, P1 and P2 domains in substrate binding, chaperoning and delivery to BAM, remain unclear [35]. Only P2 exhibits PPIase activity [30, 31], but this is dispensable *in vivo* [31]. Removal of the P2 domain (herein referred to SurA ΔP2), or deletion of both P1 and P2 (named SurA N-Ct) *in vivo* leads to only slight increases in the $\sigma^E$ stress response [31] and a small reduction in the levels of some OMPs (e.g. OmpA and LptD) [36], suggesting that these domains may be dispensible for a functional SurA *in vivo*. Indeed, many proteobacteria have SurA homologues which lack one or both PPIase domains [24]. However, a study in uropathogenic *E. coli* revealed that SurA

PPIase deletion retarded cell growth in the presence of the antibiotic novobiocin [37]. *In vitro*, while wild-type (WT) SurA is able to prevent the aggregation of the water-soluble protein, citrate synthase at 43 ℃ [31], SurA N-Ct and SurA ΔP2 displayed greater chaperone activity in the same assay, suggesting that the PPIase domains may impair the chaperone activity of SurA for this protein [31]. The role of the PPIase domains in chaperoning OMPs, however, has not been determined using *in vitro* aggregation assays to date.

Here, inspired by previous studies of SurA *in vivo* [31, 36, 37], we employed a strategy of sequential deletion of SurA PPIase domains to investigate the ability of SurA WT, SurA ΔP2 and SurA N-Ct (**Fig. 1b**) to bind and prevent the aggregation of OMPs. We selected two OMP substrates of different size: tOmpA, the 19 kDa transmembrane domain of the well-studied model OMP, OmpA [38-45], and OmpT, a 33 kDa protease [46, 47] which form 8- and 10-stranded β-barrels in their native states, respectively. Both proteins have been shown previously to be substrates for SurA *in vitro* [45, 48-50]. We show that removal of the PPIase domains has little effect on the ability of SurA to prevent the aggregation of tOmpA, consistent with previous reports that the major chaperone activity for OMPs resides in SurA N-Ct [31, 36, 37]. By contrast, removal of one or both PPIase domains ablates the ability of SurA to prevent OmpT aggregation under the conditions employed, indicating that these domains are essential for the chaperoning of at least some SurA clients. This enhanced chaperone activity of SurA variants containing two PPIase domains towards specific OMP substrates suggests a possible reason for the conservation of multiple PPIase domains in later proteobacteria.

## Results

**[51]**

### SurA homologues with two PPIase domains are enriched in β- and γ-proteobacteria

We began our investigation into the role of PPIase domains in SurA function by quantifying the distribution of SurA homologues with zero, one or two PPIase domains in different proteobacterial classes (see Methods). Sequences were obtained from the PFAM family that contain proteins with domains related to the *E. coli* SurA N-terminal domain (PF09312 - SurA_N). From the 1176 genes obtained from 1160 unique species in this dataset, those in δ-, ε-, α-, β- and γ-proteobacterial species were identified (1095 sequences). Each of these sequences was then analysed to determine the number of PPIase domains present in each SurA homologue (**Fig. 1c and Table S1**). This analysis revealed that more ancient proteobacteria (the δ-, ε- and α-classes) have SurA homologues which typically contain either one or no PPIase domains. This suggests that the ancestral SurA chaperone comprised either the core domain alone, as previously proposed [24], or the core domain with one PPIase domain. SurA homologues in later proteobacteria predominantly contain two PPIase domains, with this architecture present in 92 and 88 % of sequences from the β- and γ-classes, respectively (**Fig. 1c and Table S1**). The results indicate that two PPIase domains within SurA have been acquired and conserved during evolution, suggesting that they confer an evolutionary advantage.

**The properties of OMP sequences in early and late proteobacteria are similar**

To assess whether any single characteristic of the OMP sequences correlates with the predominance of SurA homologues containing two PPIase domains in β- and γ-proteobacteria, the properties of >350,000 predicted OMP sequences from ~6700 species in the δ-, ε-, α-, β- and γ-proteobacterial classes (**Table S2**) were analysed using data obtained from the OMPdb [52]. Specifically, the sequence length, number of β-strands, hydrophobicity, amino acid content, aggregation propensity and number of aggregation-prone regions (APRs) or aromatic-rich sequence motifs across the proteobacterial classes were compared (**Fig. 2, 3, and S1-5**). The results showed that OMPs have a broad range of sizes in each class of

proteobacteria, with no major differences observed between the distributions of sequence lengths between the proteobacterial classes (**Fig. 2**). In particular, longer sequences (e.g. >500 residues in length) are equally well represented in all classes, ruling out OMP size as the primary reason for the presence of multiple PPIase domains in SurA in the β- and γ-proteobacterial classes. Interestingly, the sequence lengths of OMPs in all classes exhibit a bimodal distribution, with peaks centred at ~350 and ~750 residues, most clearly observed in the data for the α-, β- and γ-proteobacterial classes (**Fig. 2**). This may reflect an increased relative frequency of 16-stranded porins and 22-stranded TonB-dependent transporters, respectively. Analysis of the predicted number of β-strands in the native β-barrels for each sequence (from PRED-TMBB2 predictions [53]) also showed that β-barrels with 8-26 β-strands are present in all five proteobacterial classes (**Fig. S1**).

Further, the percentage of each amino type in the OMP sequences from δ-, ε-, α-, β- and γ-proteobacteria are broadly similar to each other (**Fig. S2a**), consistent with the shared evolutionary origin of OMP sequences [54, 55]. In particular, the percentage of proline residues is not enhanced in the OMP sequences in the later proteobacterial classes (β- and γ-proteobacteria) in which multiple PPIase domains within SurA are common (**Fig. S2b and 1c**). We also examined the percentage of aromatic residues in OMP sequences from each proteobacterial class, as peptide sequences which contain aromatic motifs (Ar-Ar and Ar-X-Ar, where Ar is an aromatic residue and X is any amino acid) are known to bind SurA [19, 56, 57]. These motifs are common in OMP sequences [19] and a peptide containing an Ar-X-Ar motif (WEYIPNV) interacts with the SurA P1 domain [58]. We found that the percentage of aromatic residues is not enriched in the OMP sequences from β- and γ-proteobacteria (**Fig. S2c**). Interestingly, a slight enrichment of aromatic residues is observed in the ε-proteobacteria, compared with the other proteobacterial classes (**Fig. S2c**). We further analysed the numbers of aromatic-rich motifs (containing Ar-Ar and Ar-X-Ar sequences, see

Methods) in each OMP sequence, and found no evidence that these motifs are more prevalent in the later proteobacterial classes (β- and γ-proteobacteria) (**Fig. S3**). An enrichment in these motifs, however, is observed in the ε-proteobacteria, consistent with the greater percentage of aromatic residues in this class (**Fig. S2c and S3**). Additional analysis of the hydrophobicity scores for OMP sequences in each proteobacterial class, calculated using the Kyte-Doolittle hydrophobicity scale [59], revealed no major differences between OMPs in the different proteobacterial classes (**Fig. S4**).

Finally, we compared the aggregation propensity of OMP sequences from each proteobacterial class using the software TANGO [60], to test for possible increased aggregation propensity in the OMP sequences from β- and γ-proteobacteria, which may provide a rationale for the presence of additional PPIase domains in SurA in these classes. For each OMP sequence we examined both their TANGO aggregation scores (**Fig. 3**) and the total number of aggregation-prone regions (APRs) in each sequence (**Fig. S5**), where APRs are defined as a stretch of five or more residues with >5% β-aggregation propensity [60]. The results show no increase in aggregation propensity in the later proteobacteria. Indeed, a small reduction in aggregation propensity for OMP sequences in the β- and γ-proteobacterial classes is observed compared with those in the δ-, ε-, and α-proteobacterial classes (**Fig. 3**). Taken together, the results reveal no clear differences in the overall physico-chemical properties of OMP substrates which may explain the evolutionary addition and conservation of multiple PPIase domains in SurA homologues in β- and γ-proteobacterial species.

**The role of SurA PPIase domains in preventing OMP aggregation**

To investigate the role of the SurA core and the two PPIase domains in binding and preventing the aggregation of OMPs, we expressed, purified and characterised SurA WT, and variants in which one (SurA ΔP2) or both (SurA N-Ct) PPIase domains are deleted (**Fig. 1b**). Examination

of these proteins using far-UV circular dichroism (CD) showed that the secondary structure content of each variant closely matches that predicted, assuming that the domains fold independently to a structure similar to that observed for each domain in the WT protein (**Fig. 4a**; **Table S3**) (see Methods). A single monomeric species was observed for each variant by native electrospray ionisation mass spectrometry (ESI-MS) at 1 μM (**Fig. 4b; Table S4**), and all three variants gave rise to $^{1}H$-$^{15}N$ TROSY-HSQC NMR spectra containing narrow and well-dispersed resonances consistent with folding to a well-defined structure (**Fig. 4c**).

Next, the ability of the different SurA variants to inhibit the aggregation of tOmpA and OmpT was investigated by rapid dilution of each OMP unfolded in 8 M urea into 50 mM glycine-NaOH buffer, pH 9.5, containing 0.24 M NaCl (the latter added to induce aggregation) in the presence of different concentrations of each SurA variant. Light scattering associated with aggregation was then monitored as a function of time using nephelometry. The results showed that SurA WT retards the aggregation of both tOmpA and OmpT in a dose-dependent manner (**Figs. 5a,d, 6a,d and S6a,d**). While a 50-fold molar excess of SurA WT prevented aggregation of tOmpA (over the 30 min time period of the assay), this molar ratio was insufficient to prevent OmpT aggregation. However, aggregation of OmpT was prevented by a 100-fold molar excess of SurA WT, consistent with the greater tendency for OmpT to self-associate relative to full-length OmpA, observed in AUC experiments [61]. The kinetic competition between aggregation and weak chaperone binding between SurA and its clients (~μM affinity [45, 57]) requires a vast excess of chaperone to retard or prevent aggregation, consistent with kinetic modelling of OMP-chaperone interactions *in vivo* [62].

Importantly, tOmpA aggregation was also inhibited by SurA ΔP2 and SurA N-Ct, with a similar SurA concentration-dependence as the WT protein (**Figs. 5b,c,e,f and S6b,c**). By contrast, deletion of the P2 domain, or both PPIase domains, had a dramatic effect on the ability of SurA to prevent OmpT aggregation, with deletion of these domains removing the ability of SurA to retard aggregation (**Fig. 6b,c,e,f**). Indeed, these variants actually increased the rate

of OmpT aggregation, as measured by the decrease in $t_{50}$ (**Fig. S6b,c,e,f**), and increased the final amplitude of light scattering in a dose-dependent manner. This indicates an increase in the number and/or size of the aggregates formed, which may also involve co-aggregation of the SurA variants with OmpT (**Fig. 6b,c,e,f**).

**Binding affinities of SurA variants for OMPs correlate with aggregation prevention**

Next, microscale thermophoresis (MST) was used to measure the affinity of each SurA variant for tOmpA and OmpT. MST was performed using very low OMP concentrations (nM), ensuring their solubility in the absence of detergent or lipid [45] (Methods). These experiments showed that all three SurA variants bind tOmpA with similar affinities ($K_{d,app}$ of ~1-5 μM) (**Fig. 7a-c**; **Table S5**), in accord with previous values for OmpF and OmpG binding to SurA WT or SurA ΔP2 [57]. The ability of tOmpA to bind to SurA N-Ct demonstrates that the core region of the chaperone is sufficient for binding of this substrate. This is consistent with the observations that (1) SurA N-Ct can largely compensate for deletion of SurA *in vivo* [31, 36]; (2) SurA N-Ct can prevent the aggregation of tOmpA *in vitro* (**Fig. 5c,f**); and (3) some proteobacterial SurA homologues contain no PPIase domains (**Fig. 1c**). A different scenario is observed for the binding of the SurA variants to OmpT (**Fig. 7d-f**). While SurA WT also binds OmpT with low μM affinity ($K_{d,app}$ of 9.3 ± 0.5 μM) (**Fig. 7d**), the affinity is lower than that for tOmpA ($K_{d,app}$ of 1.8 ± 0.1 μM) (**Fig. 7a**), consistent with the greater molar excess of SurA WT required to prevent the aggregation of OmpT (compare **Figs. 5a** and **6a**). While an interaction is detected for SurA ΔP2 and SurA N-Ct binding to OmpT (**Fig. 7e,f**), as shown by a change in the normalised fluorescence signal, a full binding curve could not be obtained, presumably because the affinity is too low to saturate binding, or due to the aggregation of OmpT under these conditions, or both. Interestingly, where the data could be fitted to the Hill equation (**Fig. 7a-d**), a Hill coefficient of >1 was required to obtain an adequate fit (**Table S5**). This could indicate positive cooperativity in the interaction between multiple copies of SurA and a single

unfolded OMP chain, consistent with previous observations by native ESI-MS [45] and size exclusion chromatography [63].

**Other ATP-independent chaperones prevent aggregation of tOmpA and OmpT**

Finally, the ability of SurA to prevent the aggregation of tOmpA and OmpT was compared with the effects of two other ATP-independent *E. coli* chaperones, Trigger Factor (TF) and SecB, both of which interact with unfolded OMPs in the cytoplasm [64-66]. Aggregation assays were again performed by rapid (33-fold) dilution of tOmpA or OmpT in 8 M urea into buffer alone, or buffer containing SurA, TF, SecB, or BSA as a control (**Fig. 8a,b**). The results showed that at a 10-fold molar excess, TF and SecB significantly reduce tOmpA aggregation to an extent similar to that observed with WT SurA at the same molar excess. Interestingly, while SurA is not able to prevent OmpT aggregation when added in a 20-fold molar excess (**Fig. 6a-c**), at this concentration TF and SecB both reduce OmpT aggregation significantly, with SecB appearing to be the most efficient chaperone as judged by this assay (**Fig. 8b**). By contrast, BSA had no effect, or even slightly increased the extent of OmpT aggregation (**Fig. 8b**). Together these data indicate that SurA is less effective at preventing OmpT aggregation than the cytosolic chaperones TF and SecB. This difference is surprising given that all three chaperones are involved in OMP biogenesis during their synthesis, cytosolic transport to SecYEG and transit across the periplasm, respectively.

## Discussion

SurA plays a key role in OMP biogenesis and virulence in Gram-negative bacteria [67]. Despite the availability of crystallographic structures [34, 58], and many studies both *in vitro* [19, 31, 45, 56, 57, 63, 68-72] and *in vivo* [20, 25-28, 30, 31, 36, 73-75], the mechanism(s) by which SurA binds and chaperones its OMP clients remain(s) unknown. Previous work has shown that some SurA homologues do not contain PPIase domains [24], and a construct containing the SurA core domain alone has been shown to largely complement *ΔsurA* strains *in vivo* [31, 36, 37]. However, the significance of the multi-domain architecture of *E. coli* SurA and the roles of its individual domains in OMP biogenesis has not been resolved [35]. Here, we have investigated the role of the two PPIase domains in *E. coli* SurA using a combination of bioinformatics analyses and *in vitro* aggregation and binding experiments, utilising two model substrates OMPs with different properties, tOmpA and OmpT.

Using a bioinformatics approach we first showed that the presence of two PPIase domains is common, and conserved, in SurA homologues in β- and γ-proteobacterial species, while only one, or no, PPIase domains are generally found in earlier δ-, ε- and α-proteobacteria (**Fig. 1c**). Analysis of a large database of OMP sequences failed to reveal a clear correlation between the length, hydrophobicity, aggregation propensity, amino acid composition, or frequency of proline or aromatic-rich motifs in different proteobacterial classes and the conservation of multiple SurA PPIase domains in more recently evolved (β- and γ-) proteobacteria. Indeed, a slight decrease in aggregation propensity is observed in OMPs from the β- and γ-proteobacteria (Figs. 3 and S5), hinting that there may have been an evolutionary selection pressure to avoid aggregation that drove both an OMPome which is less prone to aggregation, and the development of better chaperones. Overall, however, the data suggest that there is no general OMP sequence property that necessitates a more complex SurA domain architecture (**Figs. 2, 3 and S1-5**). Despite this, we show here experimentally that SurA WT

displays differing chaperoning activity for tOmpA and OmpT (**Figs. 5 and 6**), with a strikingly different dependence on the presence of the two PPIase domains for the prevention of their aggregation. These results suggest that SurA may utilise different binding domains for different OMPs, with the P1 and P2 domains being required to prevent aggregation of some clients. This is consistent with the view, based on differential proteomics experiments, that SurA may play differential roles in the biogenesis of subsets of OMPs *in vivo* [27]. Experiments examining the OM proteome in cells lacking SurA found that only eight OMPs exhibited a greater than two-fold decrease in abundance in the absence of SurA (OmpA, OmpX, FadL, OmpF, LamB, FecA, FhuA, and LptD) [27]. Further, for only two of these (22-stranded FhuA (79 kDa) and 26-stranded LptD (87 kDa)) the reduction in protein level could not be explained by a $\sigma^E$ induced decrease in mRNA levels [27]. Interestingly, while data from *in vitro* studies (including herein) demonstrate that OmpT is a substrate for SurA [49, 50], the levels of OmpT observed in proteomics experiments were unaffected by deletion of SurA *in vivo* [27]. This suggests that OmpT does not require SurA for its assembly *in vivo*, and can be assisted by other proteins in the periplasmic chaperone network in the absence of SurA [9, 62, 76].

Previous analysis of the evolution of the BAM lipoproteins (BamB-E in *E. coli*), has shown that the ancestral BAM complex most likely consisted of BamA and BamD [77, 78]. BamB and BamE are largely lacking from $\delta$- and $\varepsilon$-proteobacterial species, and strikingly, no BamC homologues were detected in the $\alpha$-, $\delta$-, or $\varepsilon$-proteobacterial classes [77]. This suggests that the presence of multiple PPIase domains in SurA in later proteobacteria could have evolved to assist in delivery of OMPs to BAM complexes which contain additional subunits. Indeed, it has been shown recently that in *E. coli* strains in which OMP assembly by BAM is impaired, removal of one or both SurA PPIase domains results in a further compromised OM, as determined by a reduction in OMP levels and an increased sensitivity to detergent [36]. These findings suggest a vital role of the SurA PPIase domains in OMP folding and OM biogenesis,

at least under some biological conditions. *In vivo* work has identified different classes of OMP substrates that utilise the BAM-SurA pathway for assembly (i.e. those that are BamB-dependent, multimeric or difficult to assemble [79]). Further work focusing on OMPs spanning this broad repertoire will be necessary to determine the roles (if any) of the SurA PPIase domains in the assembly of specific sets of substrates by the BAM complex.

The large excess of SurA required to prevent aggregation of tOmpA observed here is consistent with the weak affinity of SurA and its deletion variants for this substrate ($K_d$ values in the range 0.1-10 μM for different OMP-SurA interactions [45, 57, 71] and herein). Assuming $k_{on}$ is diffusion limited (~$10^8$ $M^{-1}s^{-1}$) $k_{off}$ must be of the order of ~10-1000 $s^{-1}$, rationalising the need of an excess of SurA to compete kinetically over protein aggregation. Weak binding may provide an advantage in facilitating the release of substrate from this ATP-independent chaperone for delivery to BAM and folding into the OM. Such a mechanism of enabling substrate handover to BAM would be advantageous since it enables client release and folding in an environment lacking an external energy source, but requires many interactions with SurA (or other chaperone) molecules to prevent aggregation. These findings are consistent with previous kinetic modelling of the transport of OMPs across the periplasm which suggest that there is a dynamic reservioir of unbound chaperones in the periplasm, and that on average, each OMP makes 100's of interactions with different chaperones *en route* to the OM [62]. Moreover, it suggests that tighter binding of OMPs to SurA should reduce the requirement for an excess of chaperone to kinetically inhibit aggregation, but would block OM biogenesis by decreasing the flux of OMPs to BAM with a consequent toxic phenotype caused by accumulation of unfolded OMPs in the periplasm [80].

In conclusion, in this study we have uncovered distinct roles for the PPIase domains of SurA in preventing the aggregation of OmpT and tOmpA. The mechanistic details of how this is

achieved, for example by providing additional binding surfaces, enhancing chaperone dynamics, or helping to maintain OMPs in an extended state competent for folding [12, 35, 72] remain to be determined. The results demonstrate that the core domain of SurA endows its generic chaperone ability, while the presence of PPIase domains enhances its chaperone activity for some OMPs, suggesting one reason for the evolution and conservation of multiple PPIase domains in SurA in the β- and γ-proteobacteria. Further work with a broad range of OMPs will now be needed to investigate the determinant(s) of SurA substrate specificity and the mechanism(s) of SurA chaperone action both *in vitro*, and in the dynamic periplasmic environment.

## Materials and Methods

### Bioinformatics analysis of SurA domain conservation

Gene sequences homologous to *E. coli* SurA were obtained from the PFAM database [81]. A total of 1176 genes from 1160 unique species in the SurA_N PFAM family (PF09312) were retrieved. For each sequence the organism classification was obtained from the Uniprot database [82] and the sequences filtered to remove sequences not from δ-, ε-, α-, β- and γ-proteobacterial species, leaving 1095 sequences. Next, the sequences in each proteobacterial class were examined to determine the number of PPIase domains present. Scripts to obtain and analyse the sequence and organism classification data were all written in Python 2.7.

### Bioinformatics analysis of OMP sequences in the OMPdb

The OMPdb, containing a total of 531,456 sequences, was downloaded in text file format (http://www.ompdb.org/). To extract information for each OMP, a parser was written in Python 2.7. Each sequence record in the OMPdb contains the Uniprot ID, protein sequence, species, NCBI tax ID, predicted signal sequence (from SignalP) and topology prediction (from PRED-TMBB2), as well as database reference codes. First, the organism classification for each record was extracted from the Uniprot database using the Uniprot ID. Sequences were then filtered removing those not from δ-, ε-, α-, β- and γ-proteobacterial species, as well as those whose protein sequences contain characters other than the 20 amino acids present in proteins (860 sequences), leaving 359,456 sequences from 6749 unique species. The predicted mature sequence (i.e. following signal sequence cleavage) for each OMP was obtained by removing residues corresponding to the predicted signal sequence and used in all analyses. The predicted number of β-strands in the native state was determined from the topology prediction in the OMPdb record. To analyse the distributions of predicted number of β-strands in the native state for OMP sequences in each proteobacterial class, only sequences for which PRED-TMBB2 predicts the native state β-strand number with a >95% confidence were used.

Sections of OMP sequences containing a high density of aromatic residues have been implicated in SurA interaction from peptide binding studies [19, 56, 57]. Here, an aromatic-rich motif within an OMP sequence is defined as a sequence stretch containing only Ar-X-Ar and Ar-Ar motifs, where Ar is an aromatic reside (tryptophan, tyrosine or phenylalanine), and X is any amino acid, which is flanked on either side by two non-aromatic residues. The total number of aromatic-rich motifs were found for each OMP sequence and then divided by the sequence length to obtain the normalised number of aromatic-rich motifs per sequence. To calculate a hydrophobicity score for each OMP sequence the same method was used as in the ExPASy tool GRAVY (**gr**and **av**erage of hydrophobicit**y**). The total number of residues of each amino acid type in the sequence were found and multiplied by their respective hydropathy indices from the Kyte-Doolittle hydrophobicity scale [59]. These were then summed and divided by the length of the sequence to obtain the hydrophobicity score. To determine the aggregation propensity of each OMP sequence the software TANGO was used [60]. To calculate the number of aggregation prone regions (APRs) in each sequence, the per residue β-aggregation scores determined by TANGO were examined and the number of APRs was calculated by counting the number of stretches of at least five residues which have a β-aggregation propensity of >5% in each sequence [60]. Kruskal-Wallis and Kolmogorov-Smirnov tests were investigated to assess differences in the distributions of physico-chemical properties between proteobacterial classes. However, while many of these tests returned very small *p*-values, we considered that the underlying distributional differences were small and could be attributed to a variety of different possible causes. We concluded that significant *p*-values for small effects likely reflected the very large sample sizes involved, and were not helpful in assessing biological significance. All analyses and data plotting were performed using Python 2.7 and made use of the Numpy, Matplotlib, and Biopython libraries.

**Plasmids**

A pET28b plasmid containing the mature sequence of the *E. coli* SurA gene with an N-terminal 6xHis-tag and thrombin cleavage site was a kind gift from Daniel Kahne (Harvard University, USA) [49]. To construct the expression plasmids for the SurA ΔP2 and SurA N-Ct variants, Q5 site-directed mutagenesis (NEB, UK) was used to delete residues 281-389 or 172-389 from pET28b-SurA, respectively. The gene encoding the mature OmpT sequence was amplified from *E. coli* XL1-blue cells by polymerase chain reaction (PCR), and ligated into the pET11a plasmid using NdeI and BamHI restriction sites. The expression plasmids for tOmpA [83], SecB [84] and TF [85] were kindly provided by K. Fleming (John Hopkins University, USA), I. Collinson (University of Bristol, UK) and E. Deuerling (University of Konstanz, Germany), respectively.

**Expression and purification of His-tagged SurA and SurA variants**

His-tagged SurA was expressed and purified using a protocol adapted from Burmann *et al*. [48]. This protocol includes denaturation and refolding of the chaperone to ensure that any residual molecules bound to SurA are removed. All protein constructs were tested for refolding to the native state by CD and NMR (Fig. 4 and Table S3). The pET28b plasmid, containing the mature gene for *E. coli* SurA with an N-terminal hexa-histidine-tag and thrombin cleavage site, was transformed into *E. coli* BL21[DE3]pLysS cells (Stratagene). Cells were grown in LB (Luria-Bertani) medium containing 30 µg/ml kanamycin at 37 °C with shaking (200 r.p.m.) to an $OD_{600}$ of ~0.6. The temperature was then lowered to 20 °C and expression induced by addition of IPTG to a final concentration of 0.4 mM. Following overnight expression (~18 h), cells were harvested by centrifugation. The pelleted cells were resuspended in 25 mM Tris-HCl pH 7.2, 150 mM NaCl, 20 mM imidazole with EDTA-free protease inhibitor cocktail (Roche) for 1 hour then lysed using a cell disrupter (Constant Cell Disruption Systems, UK). Following centrifugation to remove cell debris (20 min, 4 °C, 25,000 *g*), the lysate was applied to a 5 ml HisTrap column (GE Healthcare) and washed with 25 mM Tris-HCl pH 7.2, 150 mM NaCl and 20 mM imidazole. His-tagged SurA was denatured on-column with 25 mM Tris-HCl,

6 M guanidine-HCl, pH 7.2 and eluted with a gradient of 25 mM Tris-HCl, 6 M guanidine-HCl, pH 7.2 and 500 mM imidazole. Fractions containing pure protein, judged by SDS-PAGE, were pooled and refolded by dialysis against 50 mM glycine-NaOH pH 9.5. Refolded protein was concentrated to ~200 µM using Vivaspin 20 (5 kDa MWCO) concentrators (Sartorius, UK), aliquoted, snap-frozen in liquid nitrogen and stored at −80 °C. The SurA variants SurA ΔP2 and SurA N-Ct were expressed and purified with the same method as wild-type SurA.

**Circular Dichroism**

CD spectra were acquired using a Chirascan plus CD spectrometer (Applied Photophysics) from 190–260 nm in 1 nm steps in a 1 mm path-length cell using a 2.5 nm bandwidth. Two scans were measured and averaged using SurA variants at a protein concentration of 5 µM in 50 mM glycine, pH 9.5 at 25 ℃. The secondary structure content of each variant was estimated from the CD spectra using the CDSSTR algorithm [86] at the Dichroweb server [87]. The expected percentage of α-helical and β-sheet content for the SurA variants were calculated from the structures of the domains present (PDB: 1M5Y [34]) using a script written in Python 2.7, and made use of the Biopython library and DSSP [88].

**Native electrospray ionisation (ESI) mass spectrometry**

NanoESI mass spectra of SurA WT, SurA ΔP2 and SurA N-Ct were acquired at a concentration of 1 µM in 200 mM ammonium acetate, pH 9.5 using a Synapt HDMS mass spectrometer (Waters) with platinum/gold-plated borosilicate capillaries prepared in house. Typical instrument parameters were: capillary voltage, 1.2–1.6 kV; cone voltage, 40 V; trap collision voltage, 6 V; transfer collision voltage, 10 V; trap DC bias, 20 V; backing pressure, 4.5 mbar. Data were processed with MassLynx v4.1 (Waters).

**NMR spectroscopy SurA variants**

For 2D $^{1}H^{15}N$ NMR experiments, SurA variants were labelled with $^{15}N$ by growing the bacteria in minimal HCDM1 medium supplemented with 50 µg/ml kanamycin in the presence of 1 g/l $^{15}NH_4Cl$. Proteins were purified by the same method as the $^{14}N$ SurA variants. All NMR experiments were carried out in 25 mM MES, 150 mM NaCl, pH 6.5, 5% (*v/v*) $D_2O$. Spectra were collected at 298 K on a Bruker Ascend Aeon™ 950 MHz spectrometer. The samples were prepared at 100 µM in a Shigemi 3 mm symmetrical NMR microtubes and $^{1}H$-$^{15}N$ BEST-TROSY spectra were recorded using 256 complex points in the indirect dimension, 1622 points in the direct dimension and 64 scans per increment with spectral widths of 11432 Hz and 3466 Hz in the $^{1}H$ and $^{15}N$ dimensions, respectively. WATERGATE solvent suppression was used in all experiments and NMR data were processed using NMRPipe and analysed in NMRView and CcpNmr Analysis [89-91].

**Expression and purification of tOmpA and OmpT**

tOmpA and OmpT were purified using a method adapted from [69]. Overnight cultures of *E. coli* BL21[DE3] cells (Stratagene, UK) transformed with a pET11a plasmid containing the gene sequence of the mature OMP were subcultured and grown in 500 ml LB medium containing 100 µg/ml carbenicillin at 37 °C with shaking (200 r.p.m.). When the culture reached an $OD_{600}$ of 0.6, protein expression was induced with 1 mM IPTG, and cells were harvested by centrifugation (5,000 *g*, 15 min, 4°C) after 4 hours of growth after induction. The pellet was resuspended in 50 mM Tris-HCl pH 8.0, 5 mM EDTA, 1 mM phenylmethylsulfonyl fluoride, 2 mM benzamidine for 1 hour then lysed by sonication. The insoluble fraction was collected by centrifugation (25,000 *g*, 30 min, 4°C), resuspended in 50 mM Tris-HCl pH 8.0, 2% (*v/v*) Triton X-100 and incubated for 1 hour at room temperature, with gentle agitation. The insoluble fraction was again pelleted (25,000 *g*, 30 min, 4°C) and the inclusion bodies washed twice by resuspending in 50 mM Tris-HCl pH 8.0, incubating for 1 hour at room temperature with gentle

agitation, followed by centrifugation (25,000 *g*, 30 min, 4 °C). The inclusion bodies were solubilised in 25 mM Tris-HCl, 6 M guanidine-HCl, pH 8.0 and centrifuged (20,000 *g*, 20 min, 4 °C). The supernatant was filtered (0.2 micron polyvinylidene difluoride syringe filter, Sartorius, UK) and protein purified further by gel filtration using a Superdex 75 HiLoad 26/60 column (GE Healthcare) equilibrated with 25 mM Tris-HCl, 6 M guanidine-HCl, pH 8.0. Peak fractions were concentrated to ~500 µM using Vivaspin 20 (5 kDa MWCO) concentrators (Sartorius, UK), and the protein solution then snap-frozen in liquid nitrogen and stored at −80 °C.

**Nephelometry**

tOmpA and OmpT were each buffer exchanged into 8 M urea, 50 mM glycine-NaOH, pH 9.5. Aggregation was initiated by diluting each protein to a final concentration of 2 µM protein and 0.24 M urea in 50 mM glycine-NaOH, pH 9.5 containing 0.24 M NaCl. Light scattering of 50 µL of each solution in a 96-well half area plate (Corning Product #3881) was then monitored using a Nephelostar (BMG Labtech GmbH) excited at 635 ± 10 nm with a gain of 90 over 30 min at 25 ℃. Aggregation was also measured in the same buffer containing 4 -200 µM SurA WT, SurA ΔP2 or SurA N-Ct. The signal of a buffer blank was subtracted and the minimum value in each data set was set as zero. Data were plotted in OriginPro (OriginLab).

**Microscale Thermophoresis**

Variants of tOmpA and OmpT with an N-terminal Cys were created using Q5 mutagenesis (New England Biolabs) and purified as described for the wild-type proteins. Proteins were buffer exchanged into 6 M guanidine-HCl, 50 mM Tris-HCl, pH 7.2 using 7 kDa MWCO Zeba spin desalting columns (Thermo Scientific) and diluted to a final protein concentration of 50 µM. A ten-fold molar excess of Alexa Fluor 488 C5 maleimide (Thermo Scientific) was then added and the samples incubated overnight at 4 ℃. The reaction was quenched with a 10-

fold molar excess (over Alexa Fluor 488 C5 maleimide) of β-mercaptoethanol. Protein was separated from unbound dye by size exclusion chromatography on a Superdex 200 10/300 GL column (GE healthcare) equilibrated with 6 M guanidine-HCl, 25 mM Tris-HCl, pH 7.2. Fractions containing labelled protein were concentrated using Vivaspin 20 (5 kDa MWCO) concentrators (Sartorius, UK), snap-frozen in liquid nitrogen and stored at −80 °C.

Alexa Fluor 488 labelled tOmpA or OmpT was buffer exchanged into 8 M urea, 50 mM glycine-NaOH, pH 9.5. A stock of 200 µM SurA WT/ΔP2/N-Ct in 50 mM glycine-NaOH, pH 9.5, was used to create a serial dilution (100 µM-3 nM), and Alexa Fluor 488 labelled tOmpA or OmpT was added 1:1 to give final concentrations of 100 nM OMP, 0.24 M urea in 50 mM glycine-NaOH, pH 9.5 in all samples. The samples were loaded into premium coated capillaries (NanoTemper Technologies GmbH, Germany) and measured using Monolith NT.115 (NanoTemper Tech.). Data were fitted to a Hill equation in Igor Pro (Wavemetrics):

$$S_{obs} = S_U + (S_B - S_U).\left(\frac{[L]^n}{K_D + [L]^n}\right)$$

where $S_{obs}$ is the observed signal, $S_U$ and $S_B$ are the signal of the unbound and bound state, respectively, *L* is the ligand concentration which is these experiments is the OMP and *n* is the Hill coefficient.

**Expression and purification of His-tagged Trigger Factor**

Plasmid pCA528 containing the gene for *E. coli* Trigger Factor (TF) with an N-terminal $His_6$-SUMO tag [85] was transformed into BL21(DE3) cells. Overnight cultures of these cells were subcultured and grown in LB supplemented with 40 µg/ml kanamycin at 37 °C with shaking (200 r.p.m.). After the culture reached an $OD_{600}$ of 0.6, protein expression was induced by 0.5 mM IPTG and cells grown for a further 4 hours before centrifugation. Harvested cell pellets were resuspended in lysis buffer (50 mM HEPES-KOH, pH 7.5, 150 mM KCl, 1 mM phenylmethanesulfonyl fluoride (PMSF), 5% (*v/v)* glycerol). Cells were lysed by cell disruption

and the lysate was cleared by centrifugation (30,000 *g*, 30 min, 4℃). The protein was purified using 5 ml HisTrap columns (GE Healthcare) following standard procedures. The eluted material was supplemented with $(His)_6$-Ulp1 protease (Sigma Aldrich) and dialysed overnight at 4℃ in storage buffer (25 mM HEPES-KOH, pH 7.5, 50 mM KCl, 5% (*v/v)* glycerol). The next day, liberated $(His)_6$-Sumo and $(His)_6$-Ulp1 protease were removed by flowing over a HisTrap column. The flow through containing the desired protein was then bound to an anion-exchange column (5 ml ResourceQ, GE Healthcare) and eluted with a linear gradient of NaCl in 25 mM HEPES-KOH, pH 7.5, 5% (*v/v)* glycerol. Pooled peak fractions were dialysed overnight at 4 ℃ in 50 mM HEPES-KOH, 150 mM KCl, pH 7.5, then concentrated, snap-frozen in liquid nitrogen, and stored at −80 °C.

**Expression and purification of His-tagged SecB**

*E. coli* BL21[DE3] cells (Stratagene, UK) were transformed with the plasmid pRSFDuet containing the SecB gene with a C-terminal $(His)_6$ tag. Overnight cultures of these cells were subcultured and grown in TY (Tryptone Yeast) broth supplemented with 40 μg/ml kanamycin at 37 °C with shaking (200 r.p.m.). After the culture reached an $OD_{600}$ of 0.6 protein expression was induced by 1 mM IPTG and cells grown for a further 3 hours before centrifugation. The pellet was resuspended in 20 mM Tris-HCl, 50 mM KCl, pH 7.5, then lysed using a cell disrupter (Constant Cell Disruption Systems, UK). Cell debris was then cleared by centrifugation (20 min, 4 °C, 39,000 *g*). The supernatant was filtered (0.2 micron polyvinylidene difluoride syringe filter, Sartorius, UK) then applied to a pre-equilibrated HisTrap 5ml column (GE Healthcare), washed with resuspension buffer then eluted with 330 mM imidazole. Fractions containing SecB were dialysed into 20 mM Tris-HCl, 50 mM KCl, pH 7.5 overnight then bound to a 5 ml HiTrap Q HP column (GE healthcare) pre-equilibrated with dialysis buffer. Protein was eluted with a gradient of 1 M KCl, then concentrated using Vivaspin 20 (5 kDa MWCO) concentrators (Sartorius, UK), snap-frozen in liquid nitrogen and stored at −80 °C.

**Acknowledgments**

We like to thank Karen Fleming (John Hopkins University, USA), Ian Collinson (University of Bristol, UK) and Elke Deuerling (University of Konstanz, Germany) for kindly providing the expression plasmids for tOmpA, SecB, and Trigger Factor, respectively. We are also grateful to members of the Radford and Brockwell groups for helpful advice and discussions. We further thank Nasir Khan for technical assistance. J.R.H. was funded by the US National Institutes of Health (GM102829). B.S. and A.N.C. are funded by the Biotechnology and Biological Sciences Research Council (BBSRC) (BB/N007603/1 and BB/P000037/1, respectively). A.J.H. was funded by the Wellcome Trust (105220/Z/14/Z). D.J.B. and S.E.R. are supported by the European Research Council under the European Union's Seventh Framework Programme (FP7.2007-2013/Grant agreement number 322408). The Waters Synapt G1 mass spectrometer was purchased with funding from the BBSRC (BB/E012558/1). The Chirascan plus CD spectrometer was purchased with funding from the Wellcome Trust (094232/Z/10/Z). The Monolith NT.115 MST instrument was also purchased with funding from the Wellcome Trust (105615/Z/14/Z). Calculations of OMP aggregation propensities using TANGO were undertaken using ARC3, part of the High Performance Computing facilities at the University of Leeds, UK.

**Figures and Figure Legends**

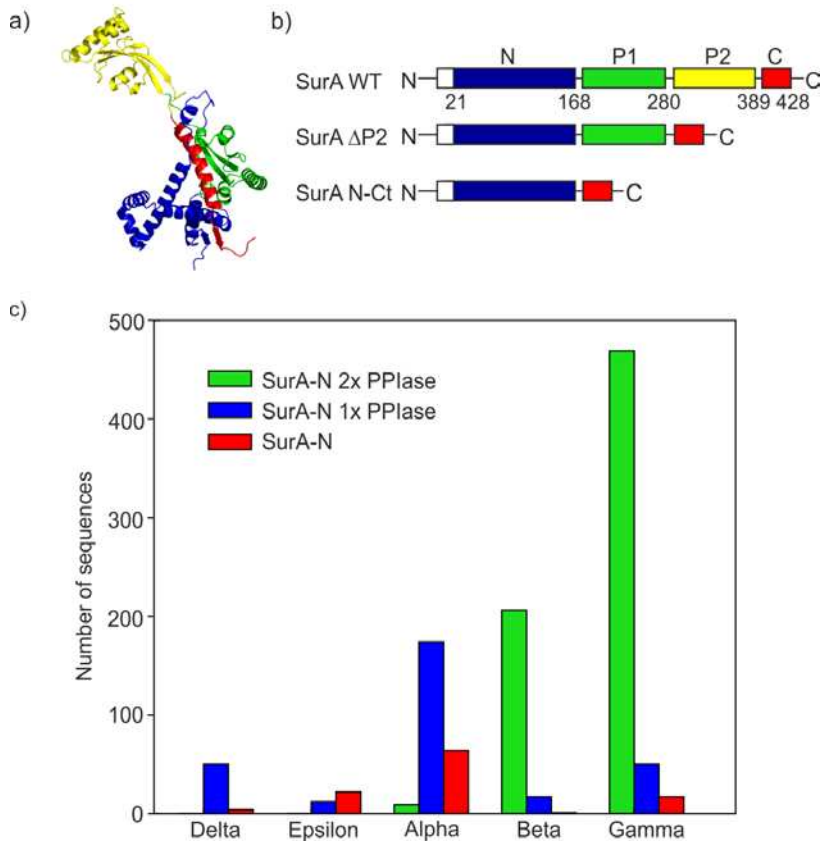


**Fig. 1** Domain architecture and evolutionary conservation of PPIase domains in SurA homologues. (a) Crystal structure of *E. coli* SurA WT (PDB: 1M5Y [34]), with missing residues added using MODELLER [51]. Domains are coloured blue (N-terminal domain), green (P1), yellow (P2) and red (C-terminal domain). (b) Schematic showing SurA variants used in this study. Domains are coloured as in (a). The signal sequence is shown in white and was not present in the constructs examined here experimentally. (c) Proteins homologous to *E. coli* SurA in δ-, ε-, α-, β- and γ-proteobacteria analysed for the presence or absence of PPIase domains. Sequences were obtained from the PFAM database and belong to the SurA_N PFAM family (PF09312).

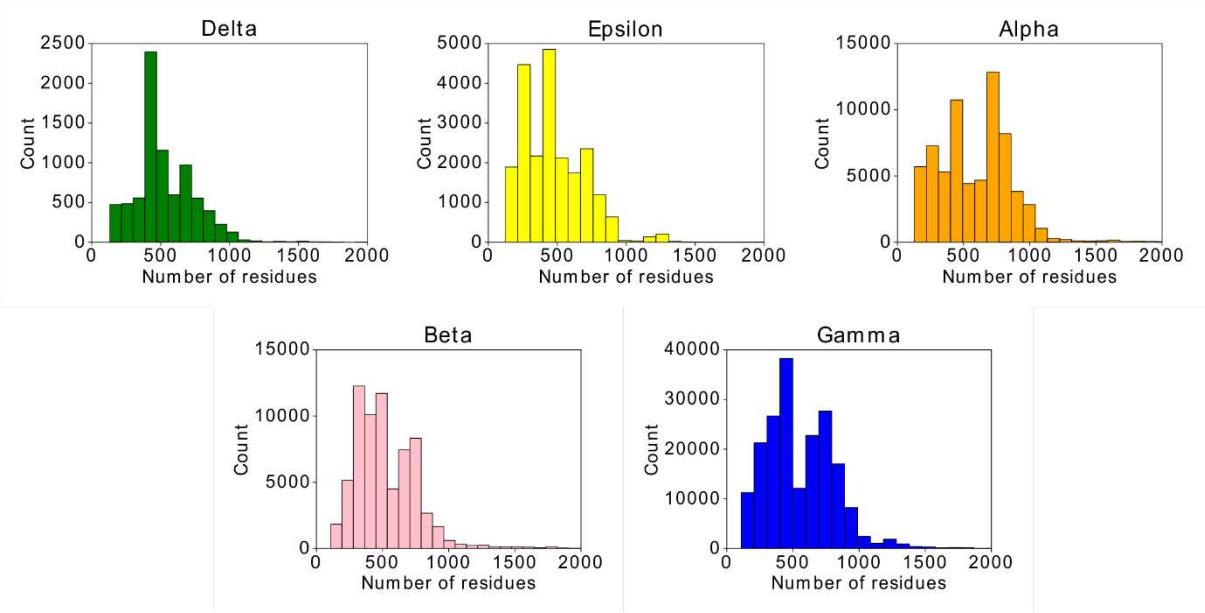


**Fig. 2**. Distributions of lengths of OMP sequences (lacking the signal sequence) in the OMPdb by proteobacterial class. No substantial differences in the range of OMP sequence lengths are observed between proteobacterial classes (see Methods).

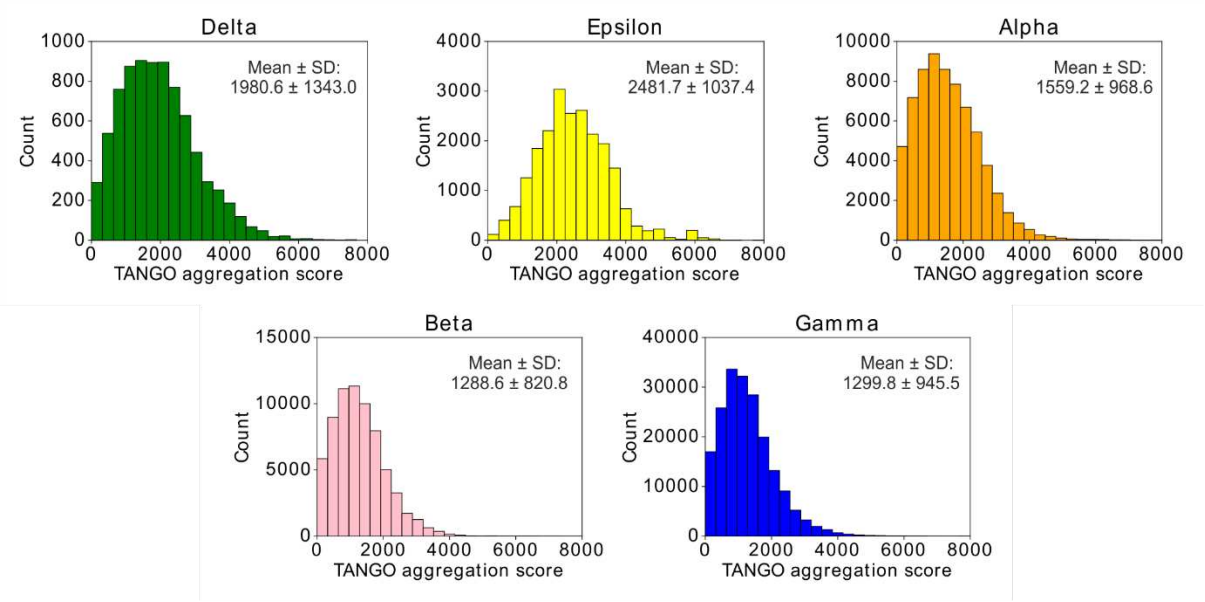


**Fig. 3**. Distributions of TANGO aggregation scores of mature OMP sequences in the OMPdb by proteobacterial class. A small reduction in aggregation propensity for OMP sequences in the β- and γ-proteobacterial classes is observed compared with those in the δ, ε-, and α-proteobacterial classes. The mean and standard deviation of TANGO aggregation scores for OMP sequences in each class are shown (see Methods). SD: standard deviation.

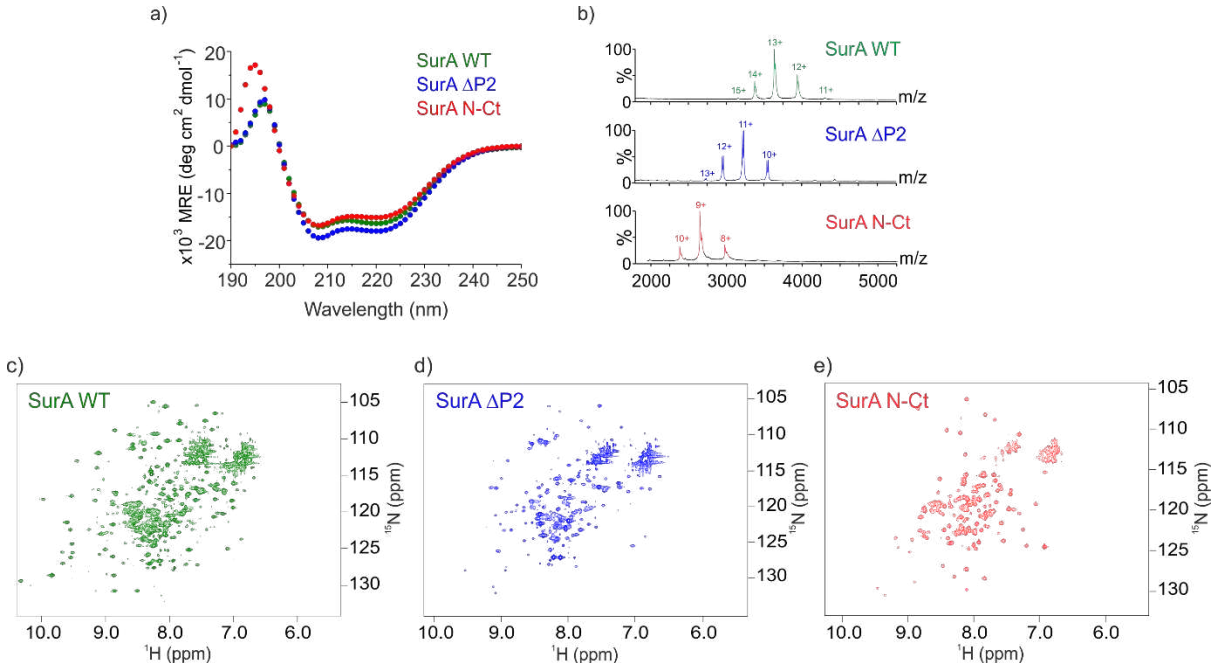


**Fig. 4.** Biophysical characterisation of SurA domain variants. (a) Far-UV CD spectra of 5 µM SurA WT (green), SurA ΔP2 (blue) and SurA N-Ct (red) in 50 mM glycine-NaOH, pH 9.5, 25° C. The predicted and observed secondary structure content of each variant is shown in **Table S3**. Similar spectra were obtained at pH 6.5 (not shown). (b) Native ESI-mass spectra of SurA variants. Samples contained 1 µM protein in 200 mM ammonium acetate, pH 9.5. Observed and expected masses for each variant are given in **Table S4**. (c-e) $^{1}H$-$^{15}N$ TROSY-HSQC spectra of (c) SurA WT, (d) SurA ΔP2 and (e) SurA N-Ct. Each spectrum contained 100 µM protein in 25 mM MES, 150 mM NaCl, pH 6.5, 25 ℃.

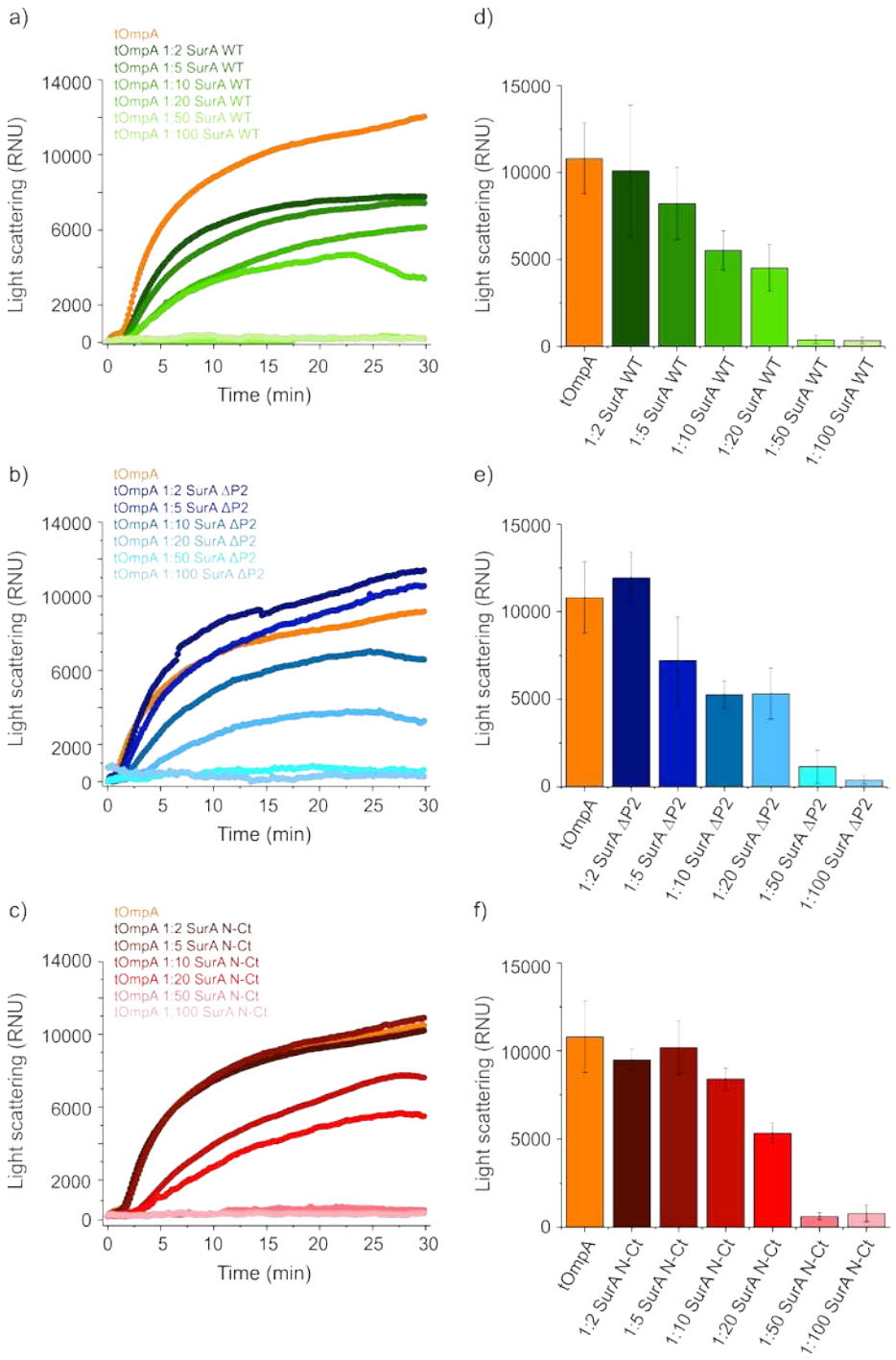


**Fig. 5.** Inhibition of tOmpA aggregation by WT and domain deletion variants of SurA. (a-c) Example aggregation reactions of tOmpA alone (orange), or in the presence of a 2-100-fold molar excess of (a) SurA WT (dark to light green); (b) SurA ΔP2 (dark to light blue), or (c) SurA N-Ct (dark to light red). (d-f) Light scattering values for aggregation assays in (a-c) at a 30 min time point. For (d-f), data are the mean and standard deviation of a minimum of three replicates for each condition. Samples contained 2 μM tOmpA, 4-200 μM SurA variant, 0.24 M urea,

0.24 M NaCl, 50 mM glycine-NaOH, pH 9.5, at 25 ℃, quiescent . RNU: Relative Nephelometry Units.

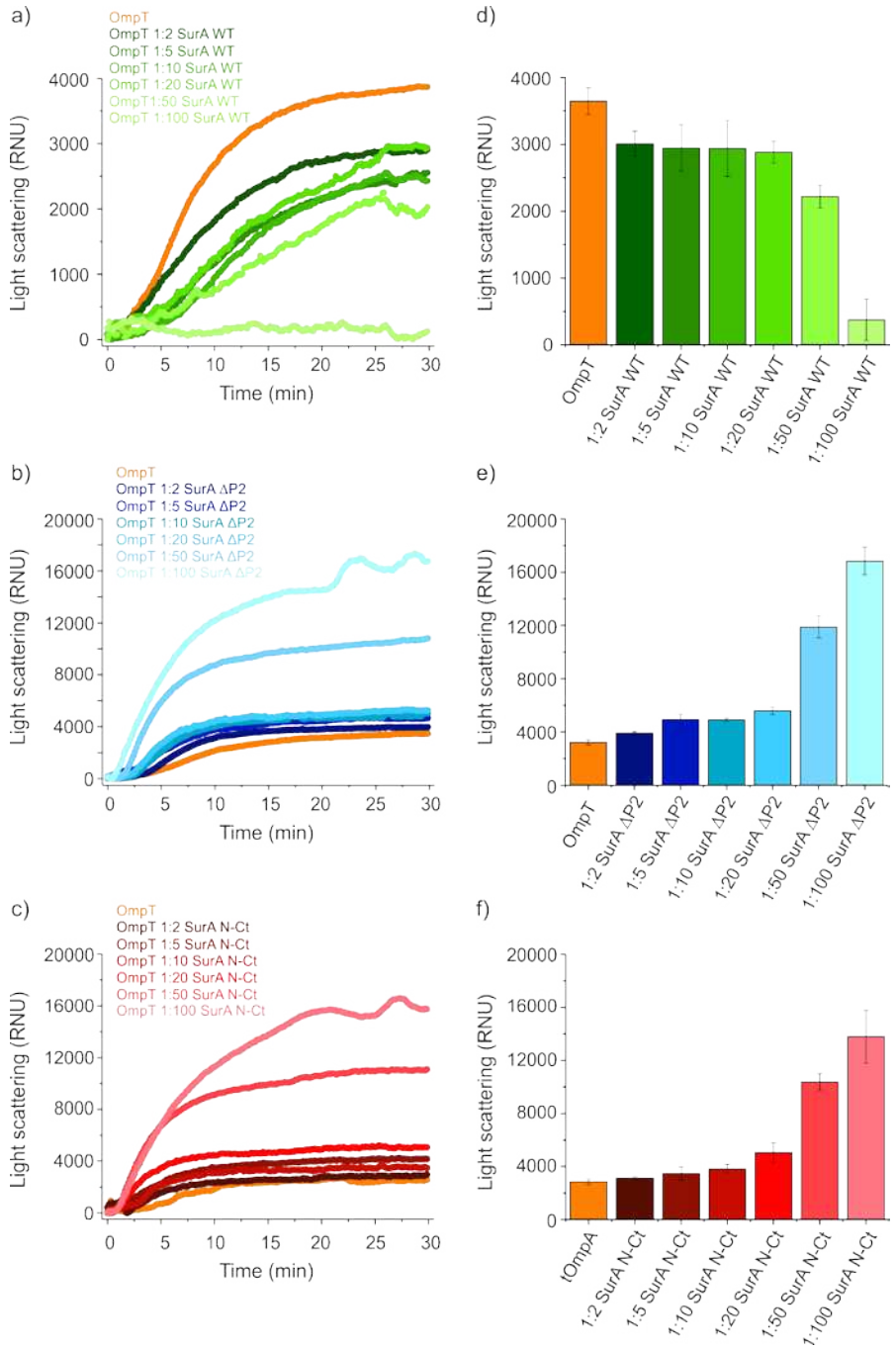


**Fig. 6.** Removal of one or both PPIase domains from SurA has a dramatic effect on its ability to prevent OmpT aggregation. (a-c) Example aggregation reactions of OmpT alone (orange), or in the presence of a 2-100-fold molar excess of (a) SurA WT (dark to light green), (b) SurA ΔP2 (dark to light blue), or (c) SurA N-Ct (dark to light red). (d-f) Light scattering values for aggregation assays in (a-c) at a 30 min time point. For (d-f), data are the mean and standard deviation of a minimum of three replicates for each condition. Samples contained 2 μM OmpT,

4-200 μM SurA variant, 0.24 M urea, 0.24 M NaCl, 50 mM glycine-NaOH, pH 9.5, at 25 ℃, quiescent. RNU: Relative Nephelometry Units.

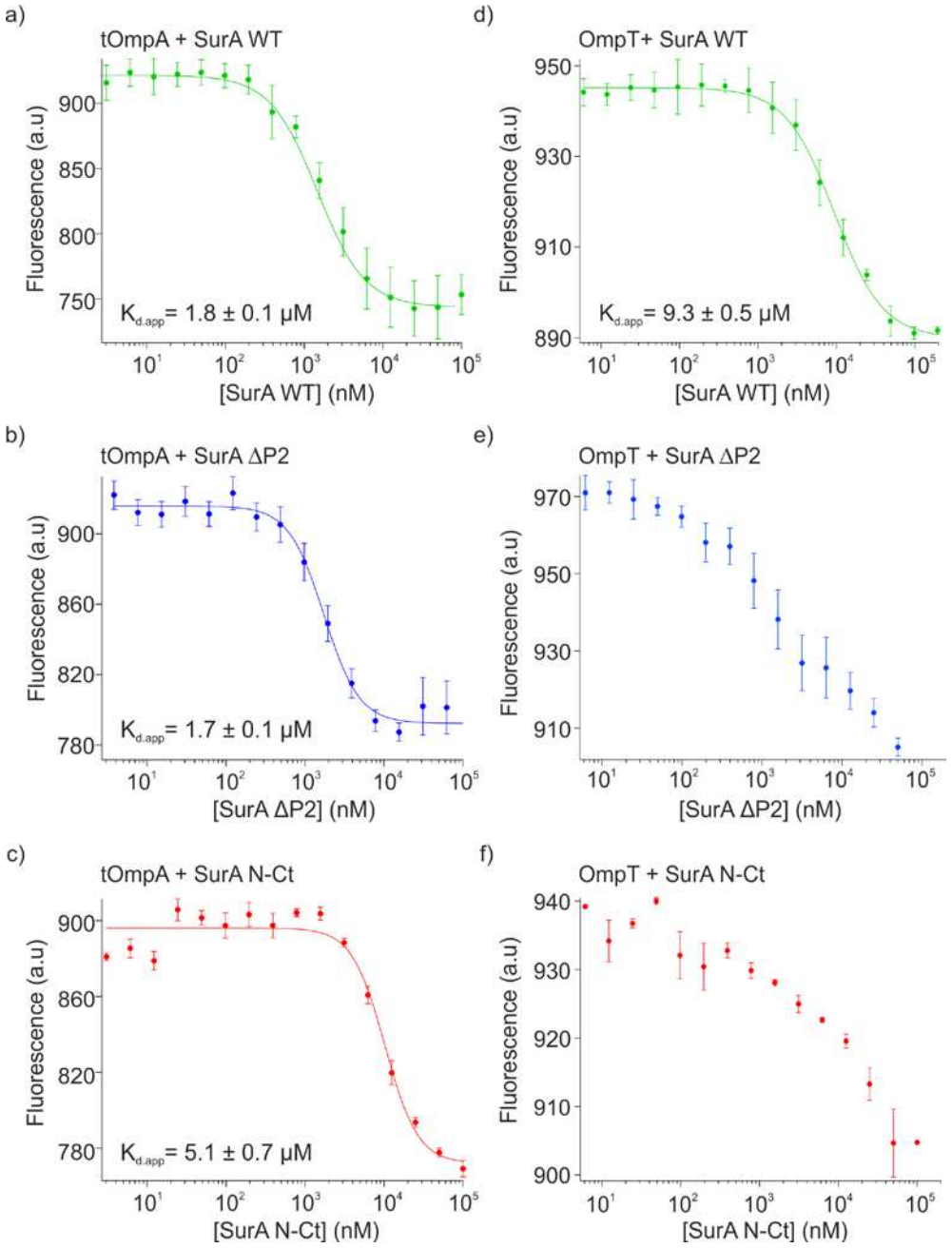


**Fig. 7.** Binding affinities of SurA variants for tOmpA and OmpT. MST binding curves for tOmpA binding to (a) SurA WT (green), (b) SurA ΔP2 (blue) and (c) SurA N-Ct (red), and for OmpT binding to (d) SurA WT (green), (b) SurA ΔP2 (blue) and (c) SurA N-Ct (red). Where possible, data were fitted to the Hill equation (shown as a solid line) (**Table S5**). Three replicates were performed and averaged (a-f) prior to fitting (a-d), and the error between replicates is plotted. Samples contained 100 nM Alexa Fluor 488-labelled OMP, 0.3 nM-100 µM SurA variant, 0.24 M urea, 50 mM glycine-NaOH, pH 9.5, at 25 ℃.

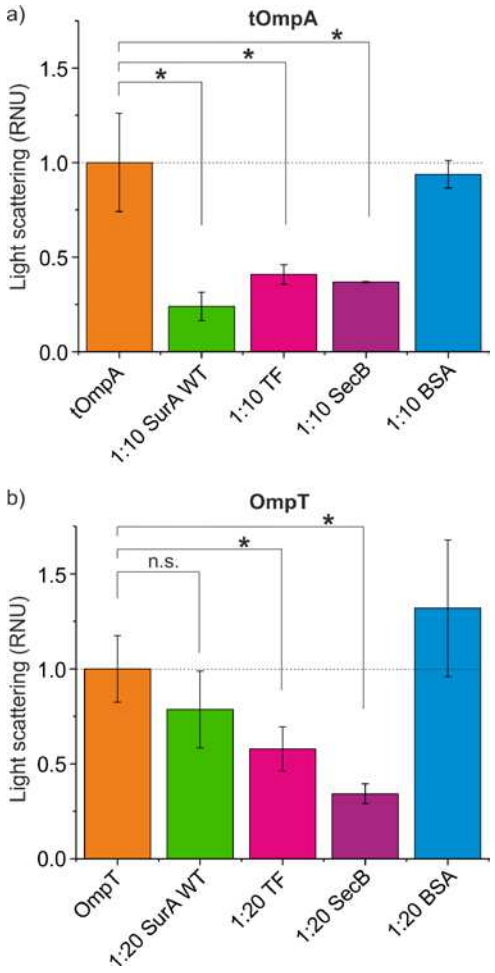


**Fig 8.** *E. coli* ATP-independent chaperones have varied effects on (a) tOmpA, and (b) OmpT aggregation. Samples contained 2 μM tOmpA/OmpT, 20 μM chaperone/BSA for tOmpA and 40 μM chaperone/BSA for OmpT, 0.24 M urea, 0.24 M NaCl, at 25 ℃. Concentrations of SecB are for the tetrameric species. Light scattering was measured by nephelometry at 635 nm following 30 min incubation at 25 ℃. Light scattering values were normalised to data obtained for OMP alone, indicated by a horizontal dotted line. Two-sample t-tests were used to test for differences in the mean light scattering values between OMP alone and chaperone containing samples. * indicates a significant difference with a *p*-value of <0.05. n.s.: non-significant. TF: Trigger Factor. RNU: Relative Nephelometry Units.

**References**

[1] Nikaido H. Molecular basis of bacterial outer membrane permeability revisited. Microbiol Mol Biol Rev. 67 (2003) 593-656.

[2] Bos MP, Robert V, Tommassen J. Biogenesis of the gram-negative bacterial outer membrane. Annu Rev Microbiol. 61 (2007) 191-214.

[3] Delcour AH. Outer membrane permeability and antibiotic resistance. Biochim Biophys Acta. 1794 (2009) 808-16.

[4] Koebnik R, Locher KP, Van Gelder P. Structure and function of bacterial outer membrane proteins: barrels in a nutshell. Mol Microbiol. 37 (2000) 239-53.

[5] Fairman JW, Noinaj N, Buchanan SK. The structural biology of β-barrel membrane proteins: a summary of recent reports. Curr Opin Struct Biol. 21 (2011) 523-31.

[6] McMorran LM, Brockwell DJ, Radford SE. Mechanistic studies of the biogenesis and folding of outer membrane proteins in vitro and in vivo: what have we learned to date? Arch Biochem Biophys. 564 (2014) 265-80.

[7] Silhavy TJ, Kahne D, Walker S. The bacterial cell envelope. Cold Spring Harb Perspect Biol. 2 (2010) a000414-a.

[8] Cross BCS, Sinning I, Luirink J, High S. Delivering proteins for export from the cytosol. Nat Rev Mol Cell Biol. 10 (2009) 255-64.

[9] Goemans C, Denoncin K, Collet JF. Folding mechanisms of periplasmic proteins. Biochim Biophys Acta Mol Cell Res. 1843 (2014) 1517-28.

[10] Wulfing C, Pluckthun A. Protein folding in the periplasm of *Escherichia coli*. Mol Microbiol. 12 (1994) 685-92.

[11] Hartl FU, Bracher A, Hayer-Hartl M. Molecular chaperones in protein folding and proteostasis. Nature. 475 (2011) 324-32.

[12] Schiffrin B, Brockwell DJ, Radford SE. Outer membrane protein folding from an energy landscape perspective. BMC Biol. 15 (2017) 123.

[13] Noinaj N, Gumbart JC, Buchanan SK. The β-barrel assembly machinery in motion. Nat Rev Micro. 15 (2017) 197-204.

[14] Knowles TJ, Scott-Tucker A, Overduin M, Henderson IR. Membrane protein architects: the role of the BAM complex in outer membrane protein assembly. Nat Rev Microbiol. 7 (2009) 206.

[15] Konovalova A, Kahne DE, Silhavy TJ. Outer membrane biogenesis. Ann Rev Microbiol. 71 (2017) 539-56.

[16] Plummer AM, Fleming KG. From chaperones to the membrane with a BAM! Trends Biochem Sci. 41 (2016) 872-82.

[17] Gessmann D, Chung YH, Danoff EJ, Plummer AM, Sandlin CW, Zaccai NR, et al. Outer membrane β-barrel protein folding is physically controlled by periplasmic lipid head groups and BamA. Proc Natl Acad Sci U S A. 111 (2014) 5878-83.
[18] Voulhoux R, Bos MP, Geurtsen J, Mols M, Tommassen J. Role of a highly conserved bacterial protein in outer membrane protein assembly. Science. 299 (2003) 262.
[19] Hennecke G, Nolte J, Volkmer-Engert R, Schneider-Mergener J, Behrens S. The periplasmic chaperone SurA exploits two features characteristic of integral outer membrane proteins for selective substrate recognition. J Biol Chem. 280 (2005) 23540-8.
[20] Sklar JG, Wu T, Kahne D, Silhavy TJ. Defining the roles of the periplasmic chaperones SurA, Skp, and DegP in *Escherichia coli*. Genes Dev. 21 (2007) 2473-84.
[21] Vuong P, Bennion D, Mantei J, Frost D, Misra R. Analysis of YfgL and YaeT interactions through bioinformatics, mutagenesis, and biochemistry. J Bacteriol. 190 (2008) 1507-17.
[22] Bennion D, Charlson ES, Coon E, Misra R. Dissection of β-barrel outer membrane protein assembly pathways through characterizing BamA POTRA 1 mutants of *Escherichia coli*. Mol Microbiol. 77 (2010) 1153-71.
[23] Gunasinghe SD, Shiota T, Stubenrauch CJ, Schulze KE, Webb CT, Fulcher AJ, et al. The WD40 protein BamB mediates coupling of BAM complexes into assembly precincts in the bacterial outer membrane. Cell Rep. 23 (2018) 2782-94.
[24] Alcock FH, Grossmann JG, Gentle IE, Likic VA, Lithgow T, Tokatlidis K. Conserved substrate binding by chaperones in the bacterial periplasm and the mitochondrial intermembrane space. Biochem J. 409 (2008) 377-87.
[25] S. Lazaar RK. SurA assists the folding of *Escherichia coli* outer membrane proteins. J Bacteriol. (1996).
[26] Ureta AR, Endres RG, Wingreen NS, Silhavy TJ. Kinetic analysis of the assembly of the outer membrane protein LamB in *Escherichia coli* mutants each lacking a secretion or targeting factor in a different cellular compartment. J Bacteriol. 189 (2007) 446-54.
[27] Vertommen D, Ruiz N, Leverrier P, Silhavy TJ, Collet JF. Characterization of the role of the *Escherichia coli* periplasmic chaperone SurA using differential proteomics. Proteomics. 9 (2009) 2432-43.
[28] Rizzitello AE, Harper JR, Silhavy TJ. Genetic evidence for parallel pathways of chaperone activity in the periplasm of *Escherichia coli*. J Bacteriol. 183 (2001) 6794-800.
[29] Justice SS, Hunstad DA, Harper JR, Duguay AR, Pinkner JS, Bann J, et al. Periplasmic peptidyl prolyl cis-trans isomerases are not essential for viability, but SurA is required for pilus biogenesis in *Escherichia coli*. J Bacteriol. 187 (2005) 7680-6.
[30] Rouviere PE, Gross CA. SurA, a periplasmic protein with peptidyl-prolyl isomerase activity, participates in the assembly of outer membrane porins. Genes Dev. 10 (1996) 3170-82.

[31] Behrens S, Maier, R. Cock, H. , Schmid, F. and Gross, C. The SurA periplasmic PPIase lacking its parvulin domains functions *in vivo* and has chaperone activity. EMBO. (2001).
[32] Palomino C, Marín E, Fernández LÁ. The Fimbrial Usher FimD Follows the SurA-BamB Pathway for Its Assembly in the Outer Membrane of *Escherichia coli*. J Bacteriol. 193 (2011) 5222.
[33] Ikenna R, Obi MSF. Demarcating SurA activities required for outer membrane targeting of *Yersinia psueudotuberculosis* adhesins. Infect Immun. 81 (2013) 2296-308.
[34] Bitto E, McKay DB. Crystallographic structure of SurA, a molecular chaperone that facilitates folding of outer membrane porins. Structure. 10 (2002) 1489-98.
[35] Mas G, Hiller S. Conformational plasticity of molecular chaperones involved in periplasmic and outer membrane protein folding. FEMS Microbiol Lett. 365 (2018) fny121.
[36] Soltes GR, Schwalm J, Ricci DP, Silhavy TJ. The activity of *Escherichia coli* chaperone SurA is regulated by conformational changes involving a parvulin domain. J Bacteriol. 198 (2016) 921-9.
[37] Watts KM, Hunstad DA. Components of SurA required for outer membrane biogenesis in uropathogenic *Escherichia coli*. PLoS One. 3 (2008) e3359.
[38] Pautsch A, Schulz GE. High-resolution structure of the OmpA membrane domain. J Mol Biol. 298 (2000) 273-82.
[39] Otzen DE, Andersen KK. Folding of outer membrane proteins. Arch Biochem Biophys. 531 (2013) 34-43.
[40] Kleinschmidt JH. Folding of β-barrel membrane proteins in lipid bilayers - Unassisted and assisted folding and insertion. Biochim Biophys Acta Biomembr. 1848 (2015) 1927-43.
[41] Chaturvedi D, Mahalakshmi R. Transmembrane β-barrels: Evolution, folding and energetics. Biochim Biophys Acta Biomembr. 1859 (2017) 2467-82.
[42] Surrey T, Jähnig F. Refolding and oriented insertion of a membrane protein into a lipid bilayer. Proc Natl Acad Sci U S A. 89 (1992) 7457.
[43] Danoff EJ, Fleming KG. The soluble, periplasmic domain of OmpA folds as an independent unit and displays chaperone activity by reducing the self-association propensity of the unfolded OmpA transmembrane β-barrel. Biophys Chem. 159 (2011) 194-204.
[44] Danoff EJ, Fleming KG. Aqueous, unfolded OmpA forms amyloid-like fibrils upon self-association. PLoS One. 10 (2015) e0132301.
[45] Schiffrin B, Calabrese AN, Higgins AJ, Humes JR, Ashcroft AE, Kalli AC, et al. Effects of periplasmic chaperones and membrane thickness on BamA-catalyzed outer-membrane protein folding. J Mol Biol. 429 (2017) 3776-92.
[46] Kramer RA, Zandwijken D, Egmond MR, Dekker N. *In vitro* folding, purification and characterization of *Escherichia coli* outer membrane protease OmpT. Eur J Biochem. 267 (2000) 885-93.

[47] Vandeputte-Rutten L, Kramer RA, Kroon J, Dekker N, Egmond MR, Gros P. Crystal structure of the outer membrane protease OmpT from *Escherichia coli* suggests a novel catalytic site. EMBO J. 20 (2001) 5033-9.
[48] Burmann BM, Wang C, Hiller S. Conformation and dynamics of the periplasmic membrane-protein-chaperone complexes OmpX-Skp and tOmpA-Skp. Nat Struct Mol Biol. 20 (2013) 1265-72.
[49] Hagan CL, Kim S, Kahne D. Reconstitution of outer membrane protein assembly from purified components. Science. 328 (2010) 890-2.
[50] Roman-Hernandez G, Peterson JH, Bernstein HD. Reconstitution of bacterial autotransporter assembly using purified components. eLife. 3 (2014) e04234-e.
[51] Eswar N, Webb B, Marti-Renom MA, Madhusudhan MS, Eramian D, Shen MY, et al. Comparative protein structure modeling using Modeller. Curr Protoc Bioinformatics. Chapter 5 (2006) Unit-5.6.
[52] Tsirigos KD, Bagos PG, Hamodrakas SJ. OMPdb: a database of β-barrel outer membrane proteins from Gram-negative bacteria. Nucleic Acids Res. 39 (2011) D324-31.
[53] Tsirigos KD, Elofsson A, Bagos PG. PRED-TMBB2: improved topology prediction and detection of β-barrel outer membrane proteins. Bioinformatics. 32 (2016) i665-i71.
[54] Remmert M, Biegert A, Linke D, Lupas AN, Soding J. Evolution of outer membrane β-barrels from an ancestral ββ hairpin. Mol Biol Evol. 27 (2010) 1348-58.
[55] Franklin MW, Nepomnyachyi S, Feehan R, Ben-Tal N, Kolodny R, Slusky JS. Evolutionary pathways of repeat protein topology in bacterial outer membrane proteins. eLife. 7 (2018) e40308.
[56] Bitto E, McKay DB. The periplasmic molecular chaperone protein SurA binds a peptide motif that is characteristic of integral outer membrane proteins. J Biol Chem. 278 (2003) 49316-22.
[57] Bitto E, McKay DB. Binding of phage-display-selected peptides to the periplasmic chaperone protein SurA mimics binding of unfolded outer membrane proteins. FEBS Lett. 568 (2004) 94-8.
[58] Xu X, Wang S, Hu YX, McKay DB. The periplasmic bacterial molecular chaperone SurA adapts its structure to bind peptides in different conformations to assert a sequence preference for aromatic residues. J Mol Biol. 373 (2007) 367-81.
[59] Kyte J, Doolittle RF. A simple method for displaying the hydropathic character of a protein. J Mol Biol. 157 (1982) 105-32.
[60] Fernandez-Escamilla A-M, Rousseau F, Schymkowitz J, Serrano L. Prediction of sequence-dependent and mutational effects on the aggregation of peptides and proteins. Nat Biotechnol. 22 (2004) 1302.

[61] Ebie Tan A, Burgess NK, DeAndrade DS, Marold JD, Fleming KG. Self-association of unfolded outer membrane proteins. Macromol Biosci. 10 (2010) 763-7.
[62] Costello SM, Plummer AM, Fleming PJ, Fleming KG. Dynamic periplasmic chaperone reservoir facilitates biogenesis of outer membrane proteins. Proc Natl Acad Sci U S A. 113 (2016) E4794-800.
[63] Thoma J, Burmann BM, Hiller S, Muller DJ. Impact of holdase chaperones Skp and SurA on the folding of β-barrel outer-membrane proteins. Nat Struct Mol Biol. 22 (2015) 795-802.
[64] Hagan CL, Silhavy TJ, Kahne D. β-Barrel membrane protein assembly by the Bam complex. Annu Rev Biochem. 80 (2011) 189-210.
[65] Oh E, Becker Annemarie H, Sandikci A, Huber D, Chaba R, Gloge F, et al. Selective ribosome profiling reveals the cotranslational chaperone action of trigger factor *in vivo*. Cell. 147 (2011) 1295-308.
[66] Lee HC, Bernstein HD. Trigger factor retards protein export in *Escherichia coli*. J Biol Chem. 277 (2002) 43527-35.
[67] Behrens-Kneip S. The role of SurA factor in outer membrane protein transport and virulence. Int J Med Microbiol. 300 (2010) 421-8.
[68] Webb HM, Ruddock LW, Marchant RJ, Jonas K, Klappa P. Interaction of the periplasmic peptidylprolyl cis-trans isomerase SurA with model peptides. The N-terminal region of SurA id essential and sufficient for peptide binding. J Biol Chem. 276 (2001) 45622-7.
[69] McMorran LM, Bartlett AI, Huysmans GH, Radford SE, Brockwell DJ. Dissecting the effects of periplasmic chaperones on the *in vitro* folding of the outer membrane protein PagP. J Mol Biol. 425 (2013) 3178-91.
[70] He L, Sharpe T, Mazur A, Hiller S. A molecular mechanism of chaperone-client recognition. Sci Adv. 2 (2016) e1601625.
[71] Wu S, Ge X, Lv Z, Zhi Z, Chang Z, Zhao XS. Interaction between bacterial outer membrane proteins and periplasmic quality control factors: a kinetic partitioning mechanism. Biochem J. 438 (2011) 505-11.
[72] Li G, He C, Bu P, Bi H, Pan S, Sun R, et al. Single-molecule detection reveals different roles of Skp and SurA as chaperones. ACS Chem Biol. 13 (2018) 1082-9.
[73] Denoncin K, Schwalm J, Vertommen D, Silhavy TJ, Collet JF. Dissecting the *Escherichia coli* periplasmic chaperone network using differential proteomics. Proteomics. 12 (2012) 1391-401.
[74] Zhong M, Ferrell B, Lu W, Chai Q, Wei Y. Insights into the function and structural flexibility of the periplasmic molecular chaperone SurA. J Bacteriol. 195 (2013) 1061-7.
[75] Ricci DP, Schwalm J, Gonzales-Cope M, Silhavy TJ. The activity and specificity of the outer membrane protein chaperone SurA are modulated by a proline isomerase domain. MBio. 4 (2013).

[76] De Geyter J, Tsirigotaki A, Orfanoudaki G, Zorzini V, Economou A, Karamanou S. Protein folding in the cell envelope of *Escherichia coli*. Nat Microbiol. 1 (2016) 16107.
[77] Anwari K, Webb CT, Poggio S, Perry AJ, Belousoff M, Celik N, et al. The evolution of new lipoprotein subunits of the bacterial outer membrane BAM complex. Mol Microbiol. 84 (2012) 832-44.
[78] Webb CT, Heinz E, Lithgow T. Evolution of the β-barrel assembly machinery. Trends Microbiol. 20 (2012) 612-20.
[79] Mahoney TF, Ricci DP, Silhavy TJ. Classifying β-barrel assembly substrates by manipulating essential Bam complex members. J Bacteriol. 198 (2016) 1984-92.
[80] Konovalova A, Grabowicz M, Balibar CJ, Malinverni JC, Painter RE, Riley D, et al. Inhibitor of intramembrane protease RseP blocks the $\sigma^E$ response causing lethal accumulation of unfolded outer membrane proteins. Proc Natl Acad Sci U S A. 115 (2018) E6614-E21.
[81] Finn RD, Coggill P, Eberhardt RY, Eddy SR, Mistry J, Mitchell AL, et al. The Pfam protein families database: towards a more sustainable future. Nucleic Acids Res. 44 (2016) D279-D85.
[82] The UniProt Consortium. UniProt: the universal protein knowledgebase. Nucleic Acids Res. 45 (2017) D158-D69.
[83] Burgess NK, Dao TP, Stanley AM, Fleming KG. β-Barrel proteins that reside in the *Escherichia coli* outer membrane *in vivo* demonstrate varied folding behavior *in vitro*. J Biol Chem. 283 (2008) 26748-58.
[84] Fessl T, Watkins D, Oatley P, Allen WJ, Corey RA, Horne J, et al. Dynamic action of the Sec machinery during initiation, protein translocation and termination. eLife. 7 (2018) e35112.
[85] Hoffmann A, Becker Annemarie H, Zachmann-Brand B, Deuerling E, Bukau B, Kramer G. Concerted action of the ribosome and the associated chaperone trigger factor confines nascent polypeptide folding. Mol Cell. 48 (2012) 63-74.
[86] Compton LA, Johnson WC. Analysis of protein circular dichroism spectra for secondary structure using a simple matrix multiplication. Anal Biochem. 155 (1986) 155-67.
[87] Whitmore L, Wallace BA. DICHROWEB, an online server for protein secondary structure analyses from circular dichroism spectroscopic data. Nucleic Acids Res. 32 (2004) W668-73.
[88] Kabsch W, Sander C. Dictionary of protein secondary structure: Pattern recognition of hydrogen-bonded and geometrical features Biopolymers. 22 (1983) 2577-637.
[89] Piotto M, Saudek V, Sklenár V. Gradient-tailored excitation for single-quantum NMR spectroscopy of aqueous solutions. J Biomol NMR. 2 (1992) 661-5.
[90] Delaglio F, Grzesiek S, Vuister GW, Zhu G, Pfeifer J, Bax A. NMRPipe: A multidimensional spectral processing system based on UNIX pipes. J Biomol NMR. 6 (1995) 277-93.

[91] Vranken WF, Boucher W, Stevens TJ, Fogh RH, Pajon A, Llinas M, et al. The CCPN data model for NMR spectroscopy: development of a software pipeline. Proteins. 59 (2005) 687-96.

## Supplementary Figures

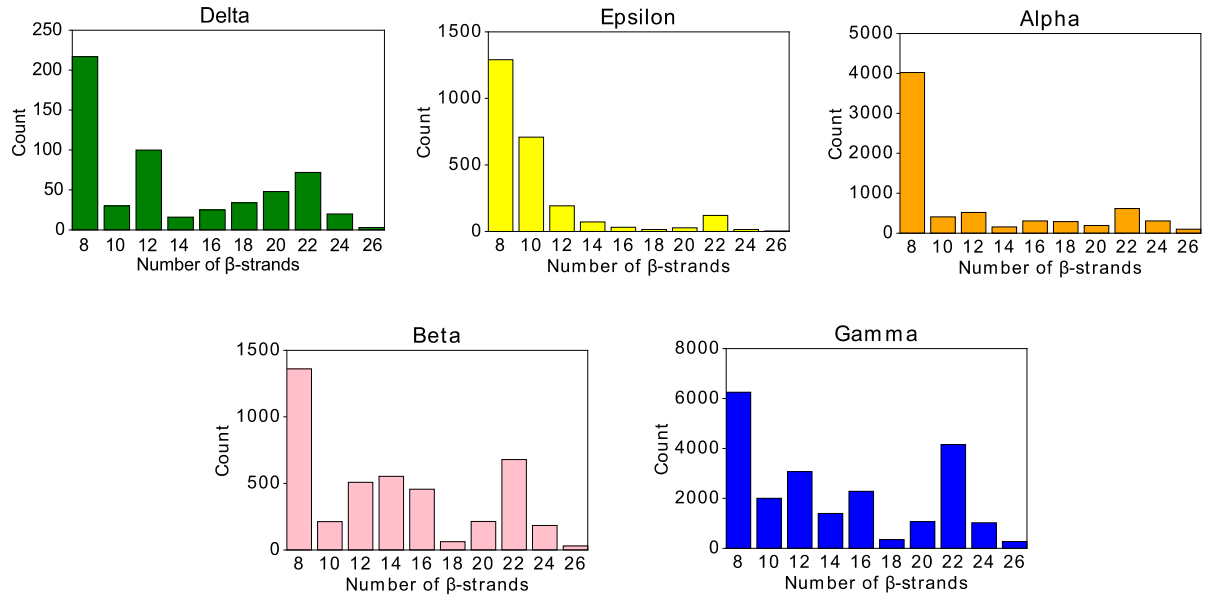


**Fig. S1**: Distributions of predicted number of β-strands in the native state of OMPs in the OMPdb by proteobacterial class. The data shown are for sequences for which PRED-TMBB2 predicts the native state β-strand number with a >95% confidence and for sizes known to be present in E. coli (8-26 β-strands).

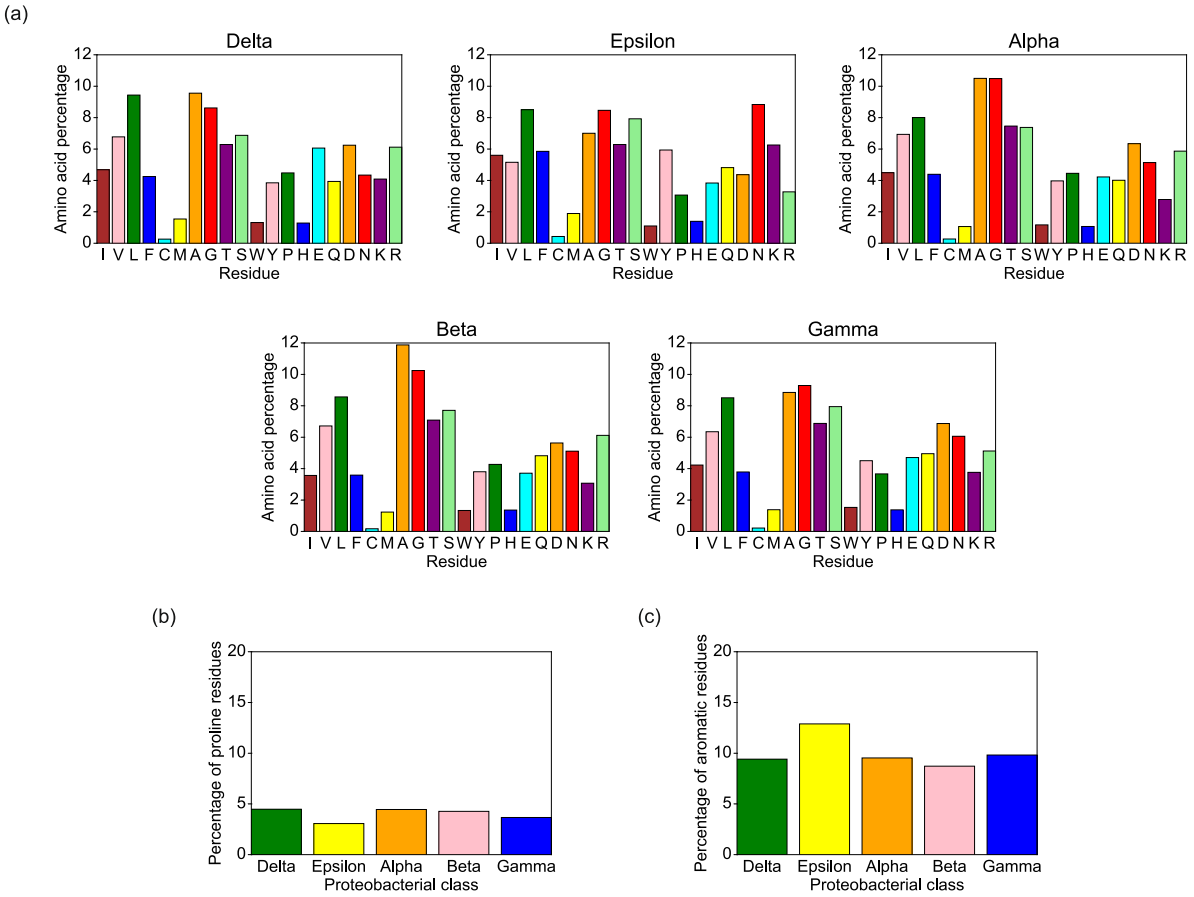


**Fig. S2**: Analysis of the amino acid content of OMP sequences in the OMPdb. Percentage of (a) all amino acid types, (b) proline residues, and (c) aromatic residues, in OMP sequences in the OMPdb by proteobacterial class.

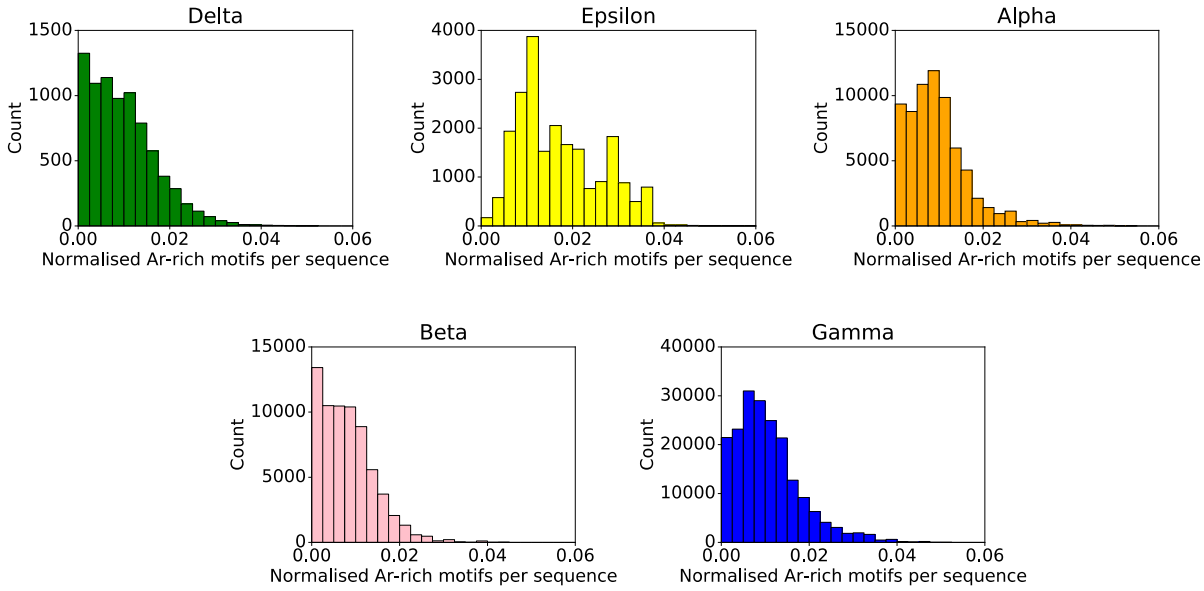


**Fig. S3**: Distributions of aromatic-rich motifs per sequence for OMP sequences in the OMPdb by proteobacterial class. The number of aromatic-rich motifs per sequence was normalised by sequence length. An aromatic-rich motif is defined as a sequence stretch containing only Ar-Ar and Ar-X-Ar sequences flanked on either side by two non-aromatic residues (see Methods). Ar: aromatic.

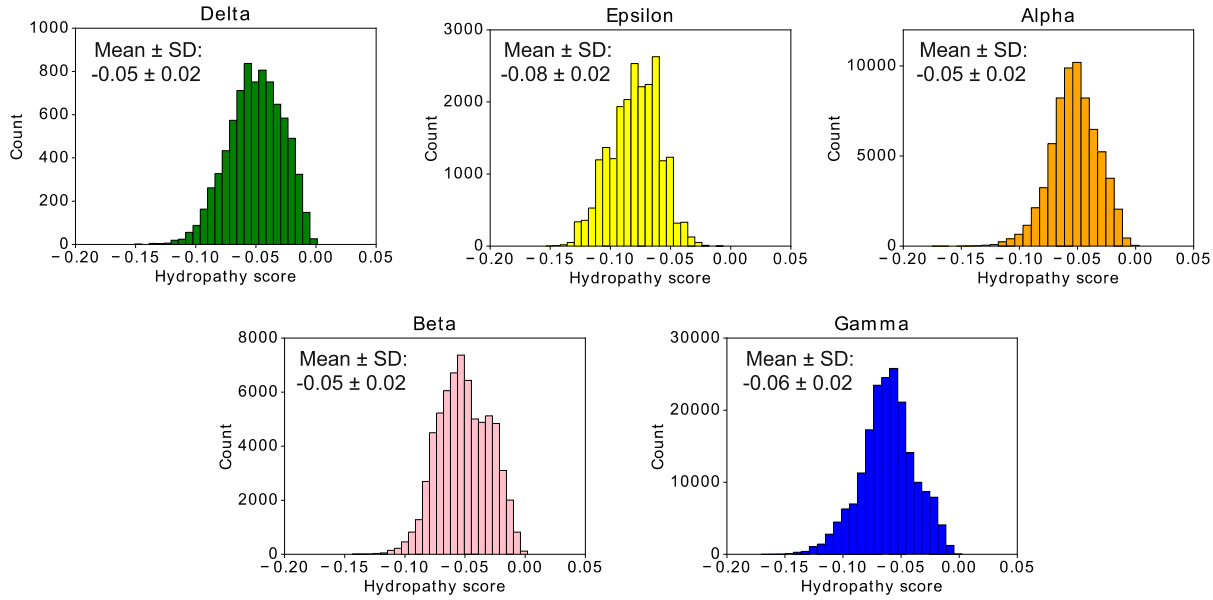


**Fig. S4**: Distributions of hydropathy scores for OMP sequences in the OMPdb by proteobacterial class. Hydropathy scores were calculated using the Kyte-Doolittle hydrophobicity scale [1]. The mean and standard deviation of hydropathy scores in each class are shown. SD: standard deviation (see Methods).

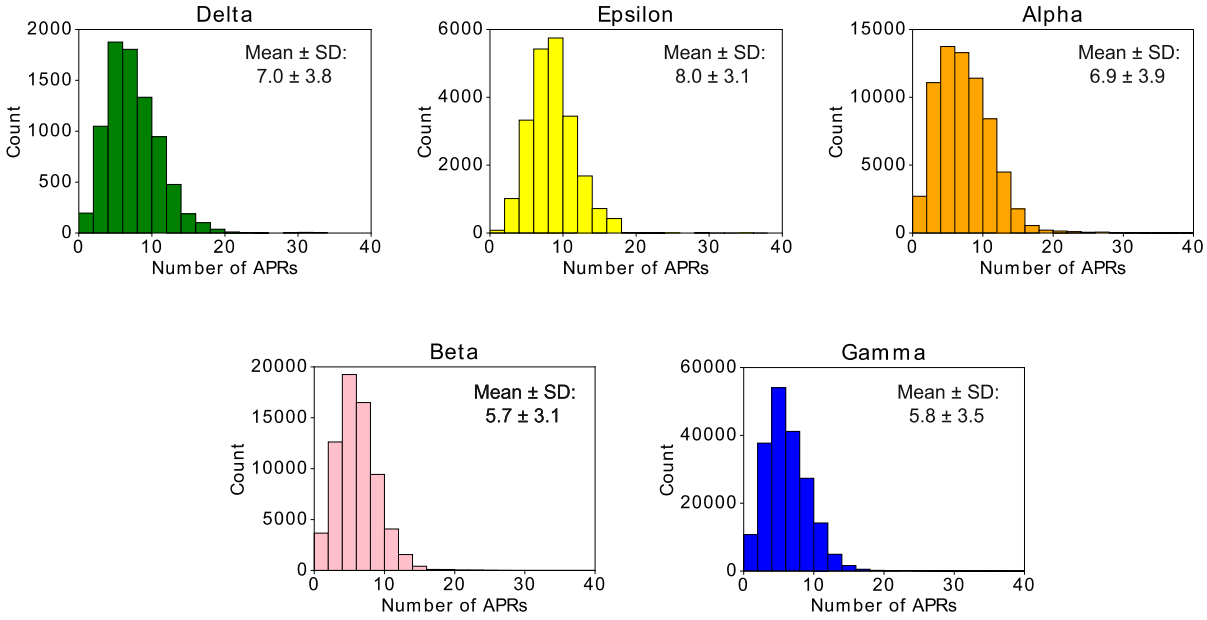


**Fig. S5**: Distributions of the number of aggregation prone regions (APRs) in OMP sequences in the OMPdb by proteobacterial class. Per residue aggregation scores were calculated using TANGO [2]. The number of APRs in each sequence was determined by counting the number of stretches of at least five residues which have a β-aggregation propensity of >5% in each sequence. The mean and standard deviation of APR numbers per sequence in each class are shown. SD: standard deviation (see Methods).

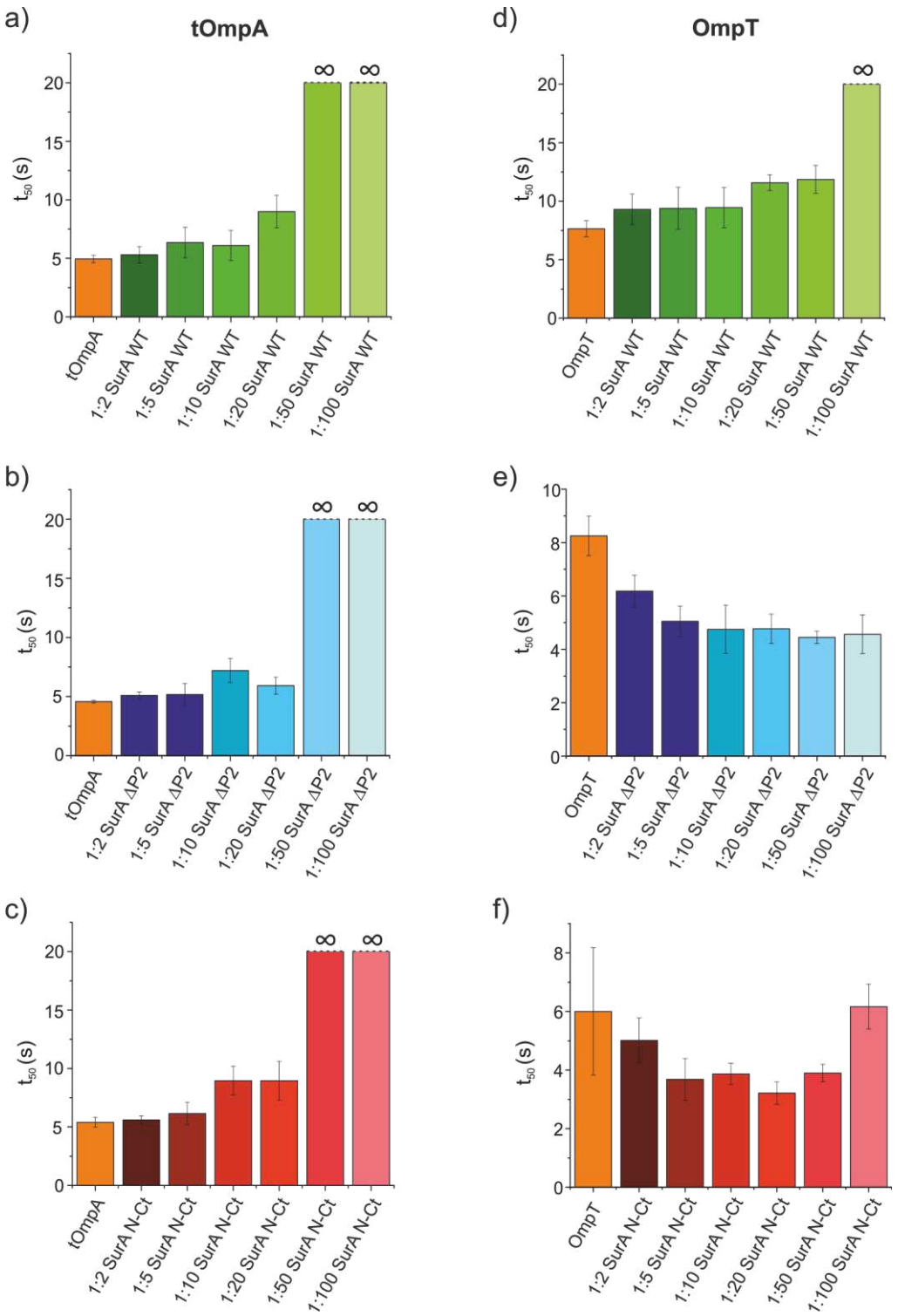


**Fig. S6.** Effects of SurA variants on the aggregation of tOmpA and OmpT. (a-c) $t_{50}$ values for aggregation assays of tOmpA alone (orange), or in the presence of a 2-100-fold molar excess of (a) SurA WT (dark to light green); (b) SurA ΔP2 (dark to light blue), or (c) SurA N-Ct (dark

to light red). (d-f) $t_{50}$ values for aggregation assays of OmpT alone (orange), or in the presence of a 2-100-fold molar excess of (d) SurA WT (dark to light green); (e) SurA ΔP2 (dark to light blue), or (f) SurA N-Ct (dark to light red). The mean and standard deviation of a minimum of three replicates for each condition. Conditions highlighted by an infinity symbol (∞) indicate those in which no aggregation was detected over the experimental timescale (30 min). Samples contained 2 μM tOmpA/OmpT, 4-200 μM SurA variant, 0.24 M urea, 0.24 M NaCl, 50 mM glycine-NaOH, pH 9.5, at 25 ℃, quiescent.

**Supplementary Tables**

| Proteobacterial class | Number of PPIase domains | Number of sequences | Percentage (%) |
|---|---|---|---|
| Delta | 0 | 4 | 7 |
| | 1 | 50 | 93 |
| | 2 | 0 | 0 |
| Epsilon | 0 | 22 | 65 |
| | 1 | 12 | 35 |
| | 2 | 0 | 0 |
| Alpha | 0 | 64 | 26 |
| | 1 | 174 | 70 |
| | 2 | 9 | 4 |
| Beta | 0 | 1 | 0.5 |
| | 1 | 17 | 7.5 |
| | 2 | 206 | 92 |
| Gamma | 0 | 17 | 3 |
| | 1 | 50 | 9 |
| | 2 | 469 | 88 |

**Table S1**: Analysis of the number of PPIase domains in SurA sequences homologous to E. coli SurA in $\delta$-, $\varepsilon$-, $\alpha$-, $\beta$- and $\gamma$-proteobacteria. Sequences were obtained from the PFAM database and belong to the SurA_N PFAM family (PF09312).

| Proteobacterial class | Number of sequences in OMPdb | Number of species |
|---|---|---|
| Delta | 8045 | 363 |
| Epsilon | 21906 | 397 |
| Alpha | 68155 | 2027 |
| Beta | 67926 | 902 |
| Gamma | 193424 | 3060 |

**Table S2**: Number of OMP sequences and species in the OMPdb from δ, ε-, α-, β- and γ-proteobacteria.

| Protein | Method | % Helix | % β-sheet |
|---|---|---|---|
| SurA WT | Calculated | 46 | 18 |
| | Far-UV CD | 50 | 18 |
| SurA ΔP2 | Calculated | 53 | 14 |
| | Far-UV CD | 57 | 14 |
| SurA NCt | Calculated | 64 | 5 |
| | Far-UV CD | 61 | 9 |

**Table S3**: The secondary structure content of SurA variants measured by far-UV CD spectroscopy closely match those calculated from the crystal structure of SurA WT (PDB: 1M5Y [3]). Percentages of helical and β-sheet content of each variant were calculated from the structures of the domains present using DSSP [4]. The CDDSTR algorithm [5] at the Dichroweb server [6] was used to estimate the secondary structure content from far-UV CD spectra of the SurA variants (**Fig. 4a**).

| Protein | Expected Mass (Da) | Observed Mass (Da) |
|---|---|---|
| SurA WT | 47,241 | 47,259 ± 3 |
| SurA ΔP2 | 35,375 | 35,394 ± 0.5 |
| SurA N-Ct | 23,799 | 23,800 ± 3.5 |

**Table S4**: Observed and expected masses of SurA variants measured by native ESI-MS. The mass spectrometry conditions were optimised empirically for each sample to maintain the protein in a folded conformation and to decrease peak widths by increasing the cone voltage and trap collision energy, (typically 100 V and 10 V, respectively). Differences in the observed and predicted masses are likely due to salt adducts which are not removed under the gentle conditions used.

| | SurA WT | | SurA ΔP2 | | SurA N-Ct | |
|---|---|---|---|---|---|---|
| | $K_d$ (μM) | Hill coeff. | $K_d$ (μM) | Hill coeff. | $K_d$ (μM) | Hill coeff. |
| **tOmpA** | 1.8 ± 0.1 | 1.4 ± 0.1 | 1.7 ± 0.1 | 1.9 ± 0.2 | 5.1 ± 0.7 | 2.1 ±0.5 |
| **OmpT** | 9.3 ± 0.5 | 1.3 ± 0.1 | N/A | N/A | N/A | N/A |

**Table S5**: Binding affinities of tOmpA and OmpT to SurA variants measured by MST. Each interaction was measured in triplicate and data points averaged prior to fitting. Data were fitted to the Hill equation (see Methods) and reported errors from the fit of three averaged traces. N/A: Not applicable. Coeff: coefficient

## References


[1] Kyte J, Doolittle RF. A simple method for displaying the hydropathic character of a protein. J Mol Biol. 157 (1982) 105-32.

[2] Fernandez-Escamilla A-M, Rousseau F, Schymkowitz J, Serrano L. Prediction of sequence-dependent and mutational effects on the aggregation of peptides and proteins. Nat Biotechnol. 22 (2004) 1302.

[3] Bitto E, McKay DB. Crystallographic structure of SurA, a molecular chaperone that facilitates folding of outer membrane porins. Structure. 10 (2002) 1489-98.

[4] Kabsch W, Sander C. Dictionary of Protein Secondary Structure: Pattern Recognition of Hydrogen-Bonded and Geometrical Features Biopolymers. 22 (1983) 2577-637.

[5] Compton LA, Johnson WC. Analysis of Protein Circular Dichroism Spectra for Secondary Structure Using a Simple Matrix Multiplication. Anal Biochem. 155 (1986) 155-67.

[6] Whitmore L, Wallace BA. DICHROWEB, an online server for protein secondary structure analyses from circular dichroism spectroscopic data. Nucleic Acids Res. 32 (2004) W668-73.